Organic Linker Design for Control of Metal-Organic Nanotube Pore Size

A Thesis Presented for the

Master of Science

Degree

The University of Tennessee, Knoxville

Patrick Flavin Luciani

December 2024

DEDICATION

I would like to dedicate this thesis to my father, Mr. John Mario Luciani. It was he who inspired me to never run from a challenge and to have the strength to stand proud at the end of each day.

ACKNOWLEDGEMENTS

I would like to first thank my advisor, Dr. David Jenkins, for his support and guidance facilitated both my academic growth as a student and my personal growth as an individual. While a graduate student at the University of Tennessee I had the utmost privilege to be under the guidance of many mentors who shaped me into the man I am today, but I would not have become the scientist I am now without his words of wisdom. The moments that I shared while in his group taught me great meanings of camaraderie and provided me a space of positivity to grow. I would also like to extend my thanks to Dr. George Schweitzer for teaching me the fundamentals of inorganic chemistry and always providing me with laughs and advice whenever needed.

I must also extend my thanks to Dr. Phattananawee Nalaoh who imparted me with wisdom on crystallography, organic synthesis, and many other heartfelt moments where I was supported when I had become lost or confused in my own research. I also need to include special thanks to Dr. Kevin Blatchford who helped to instill in me the importance of learning the fundamentals, focusing on the importance of time management, and providing me with an ideal role model for becoming an excellent inorganic chemist. To Nick Orlando, my time as a graduate student would not have been the same without you. I value our friendship, the many nights spent slamming down energy drinks where we rattled ideas off one another, and as always, our similar sense of humor that always picked me up when I was frustrated. To Henry Brothers, your brilliance in the lab is what inspired me to take steps toward trying to shine as brightly as you. To the rest of the Jenkins group, thank you for your support, the laughs, the conversations, and helping to elevate me to greater heights.

ABSTRACT

Metal-Organic Nanotubes (MONTs) are a crystalline one-dimensional porous material that can be formed from the interaction between an organic ligand and a metal. The synthesis of this class of material is similar to its three-dimensional counterpart (MOFs) where in both cases precise choice of ligand and metal can result in the altering of material dimensions. When highlighting the differences between these two classes of coordination polymers, the exploration of MONTs has shown that they are formed anisotropically in which their one-dimensional growth causes them to be a functionally successful choice for the adjustment of organic linker synthesis and size.

Within our group, there have been many different avenues in which MONTs as a material have been investigated. MONTs have been prepared utilizing a 2, 3, and 4 column pillared approach where herein the Jenkins group the 2-column pillared approach is utilized. With the work done by the Jenkins group in the both the past and in the present, there have been a series of organic linkers specifically designed to investigate the relationship between a semi-ridgid di-triazole organic linker and an associated metal of which has generally been copper or silver. Expanding on the research of previous group members and herein this thesis, a review of particle size, composition, and more importantly, pore size is discussed.

In the past, the goal of this research group has been to identify and rationalize the ideal way to synthesize these discrete nanotubes on the bulk scale. Although this goal is still present to this day, a goal that is more pressing is highlighted within this thesis. To highlight specifically, the goal of the research herein this thesis is to accomplish the synthesis of MONTs utilizing expanded organic linkers of which could form a novel crystalline material with an expanded pore. Through the utilization of collaborations in the field, different techniques using

crystallography as the basis were employed in order to fully characterize the synthesized expanded MONTs as a material.

TABLE OF CONTENTS

LIST OF TABLES

LIST OF FIGURES

CHAPTER 1

INTRODUCTION

The properties and applications of any material are dictated by its dimensionality. One-dimensional materials exploded onto the scene in 1991 when Sumio Iijima pioneered the synthesis of carbon nanotubes (CNs). [1] Carbon nanotubes can be broken into two primary classes, of which are single-walled carbon nanotubes (SWCNTs) and multi-walled carbon nanotubes (MWCNTs) (***Figure 1***).[1]

While each class behaves in many similar ways, the main point for discussion is how they are defined. These anisotropic materials are defined by their one dimensional growth along one axis and are most well known for having both high tensile strength and their applications in electronics. [2-4] Applying fundamental knowledge of dimensionality, structural modifications that directly reflect these concepts can be studied when looking at inorganic materials. Metal-organic frameworks (MOFs) are within a class of materials which are commonly referred to as coordination polymers.[8,10-11] MOFs pioneered by Omar Yaghi follow a pattern of growth where they can be found in one, two, or three-dimensions. [24,25] With large, interconnected pores, MOFs are best known for having successful developments in gas storage, heterogenous catalysis, and chemical separations (***Figure 2***).[8]

In 2008, Daofeng Sun prepared a new subtype of coordination polymer which was given the name Metal-Organic Nanotubes (MONTs).[23] Metal-Organic Nanotubes are a type of MOF which encompasses not only the desirable qualities that are found in their multi-dimensional counterparts but also includes desirable qualities found in CNs.[5-7,13] When fusing the qualities of each of these materials together a material is born that has an adjustable pore size, increased flexibility, and potential for exterior functionalization post-synthesis.[5]

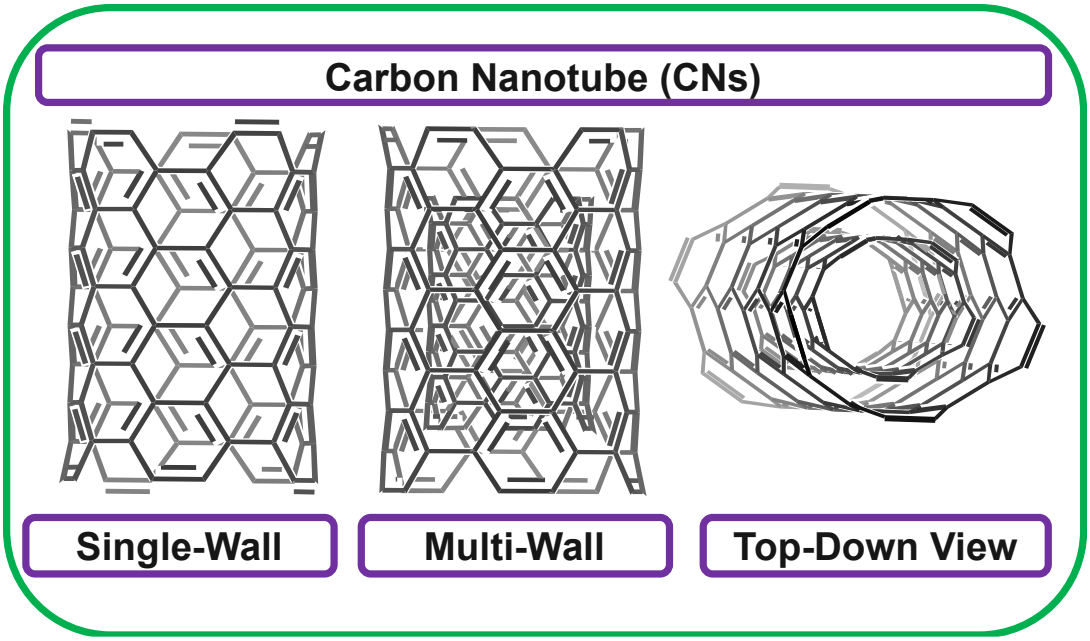

Figure 1. **Carbon nanotube formation is characterized based on a pair of integers which describe the orientation and diameter of the nanotube. These can be seen as either SWCNTs or MWCNTs where the appropriate nomenclature labels the x-axis as "armchair" and the y-axis is as "zigzag".**

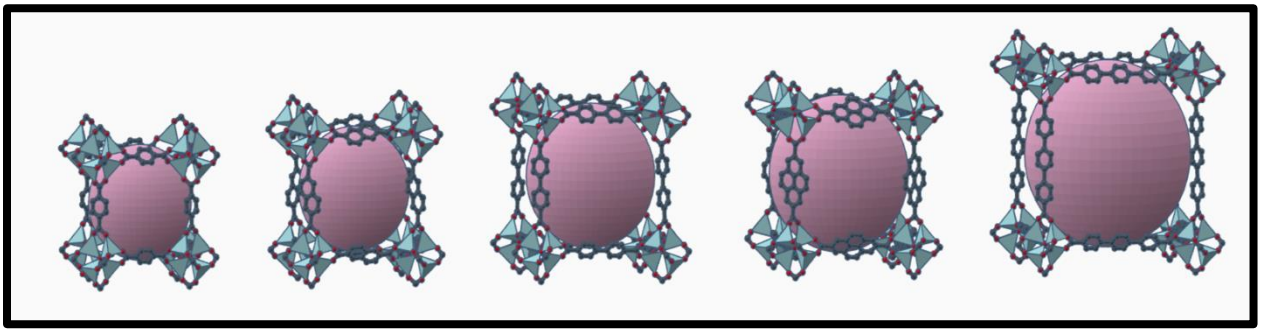

Figure 2. **As more MOFs were synthesized, Dr. Ohmar Yaghi pioneered the first concepts of isoreticularity which demonstrated that with the altering of an organic ligand the chemical environment and size of the pore could be changed.**

Made typically under solvothermal conditions, MOFs and MONTs are made from carefully selecting an organic linker and pairing it with a metal salt.[5] Through many different combinations, there are hundreds of thousands of avenues from which new metal organic materials can be synthesized. In 2003, Ohmar Yaghi pioneered the discovery of isoreticularity where two MOFs could differ in pore size, metal selection and function, but still maintain the same underlying pore topology. With this principle in mind, our research group was the first to develop isoreticular synthesis of MONTs.[24-25] With this discovery, our research group began looking into the effects of how pore size may affect synthesis, how copolymerization may be possible, and how selection of ligand could influence pi-pi interactions (***Figure 3)***.

Within the last decade MONTs have been synthesized in multiple different ways with the primary three being the two-column pillared approach, the three-column pillared approach and the four-column pillared approach.[5] In 2011, Hiroshi Kitagawa was the first to synthesize a four-column pillared MONT. This was accomplished by reacting the square-shaped metal-organic building block $[Pt(en)(bpy)]_4(NO_3)8{\cdot}5H_2O$ with iodine and undergoing an oxidative polymerization in order to form $[Pt(en)(bpy)I]_4(NO_3)_8 \cdot 16H_2O$.[6] With these specific MONT growth conditions, both the height and the width had a requirement of being adjusted at the same time in order to propagate formation (***Figure 4***).[6]

Many years later, Ben-Lai Wu synthesized the first three-column pillared MONT which boasted one of the most complex ways to form MONTs. This feat was accomplished by the reaction of two organic linkers and a metal salt. To specify, 1,1'-(5-methyl-1,3-phenylene)bis(1H-imidazole), 5-bromonicotinate (Brna), and a nickel salt were carefully selected to orchestrate the formation of this MONT.[5] (***Figure 5)***

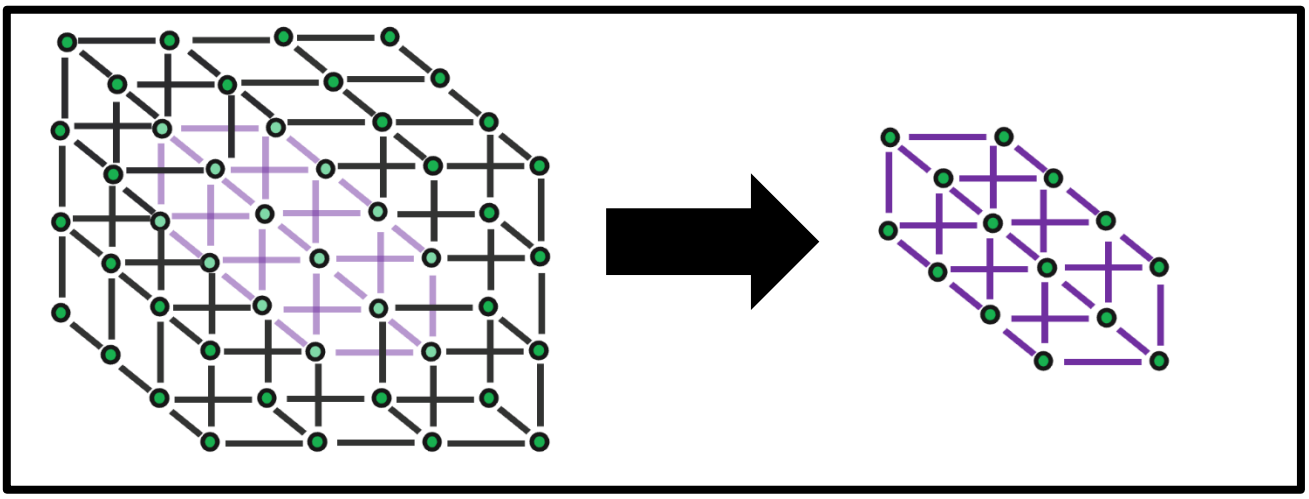

Figure 3. **MOFs and MONTs are both a class of coordination polymer with the primary difference being pattern of growth. MOFs can grow in 2, or 3 dimensions whereas MONTs are grown ideally in 1 direction. Within our research group, highlighting isoreticularity allowed for the development and growth of many different MONTs.**

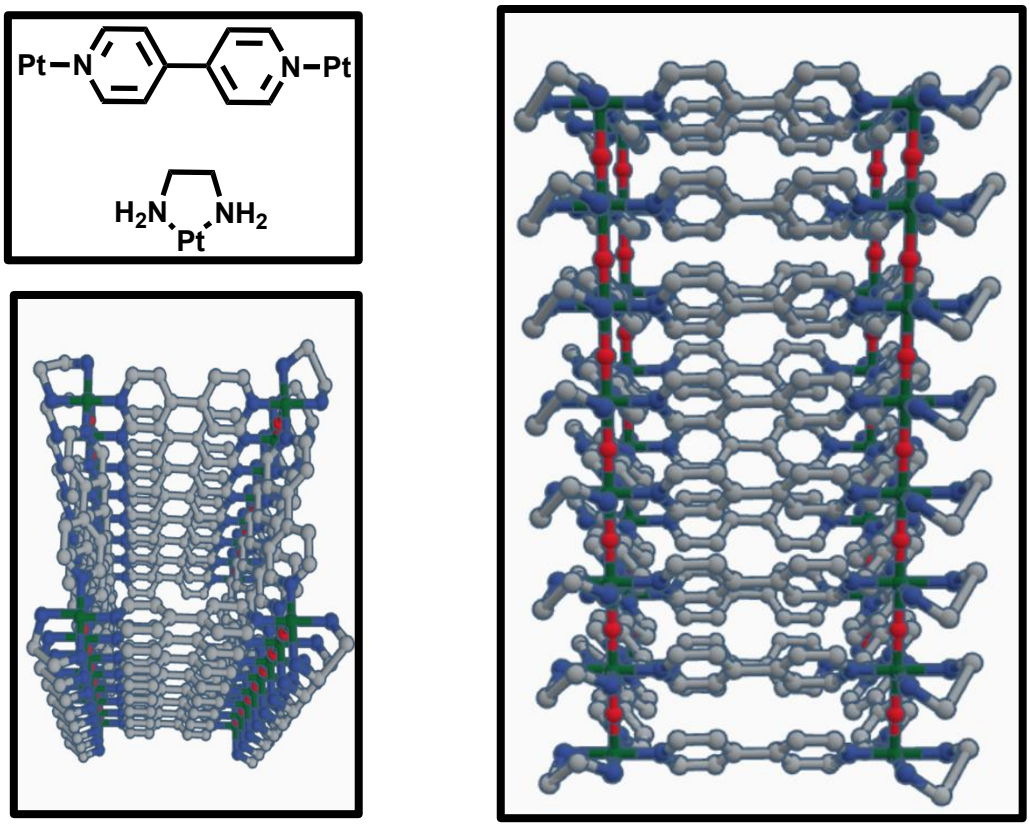

Figure 4. **(a). Ethylenediamine and 4,4'-bipyridine coordinating to a platinum center. (b). Top and (c). side facing views for the four-column pillared MONT $[Pt(en)(bpy)I]_4(NO_3)_8 \cdot 16H_2O$. MONTs synthesized in the Kitagawa group use an anionic iodine which act as a bridging within the four-column pillar. Similar to other MONTs a capping agent, in this case ethylenediamine is used to "close" the pore.**

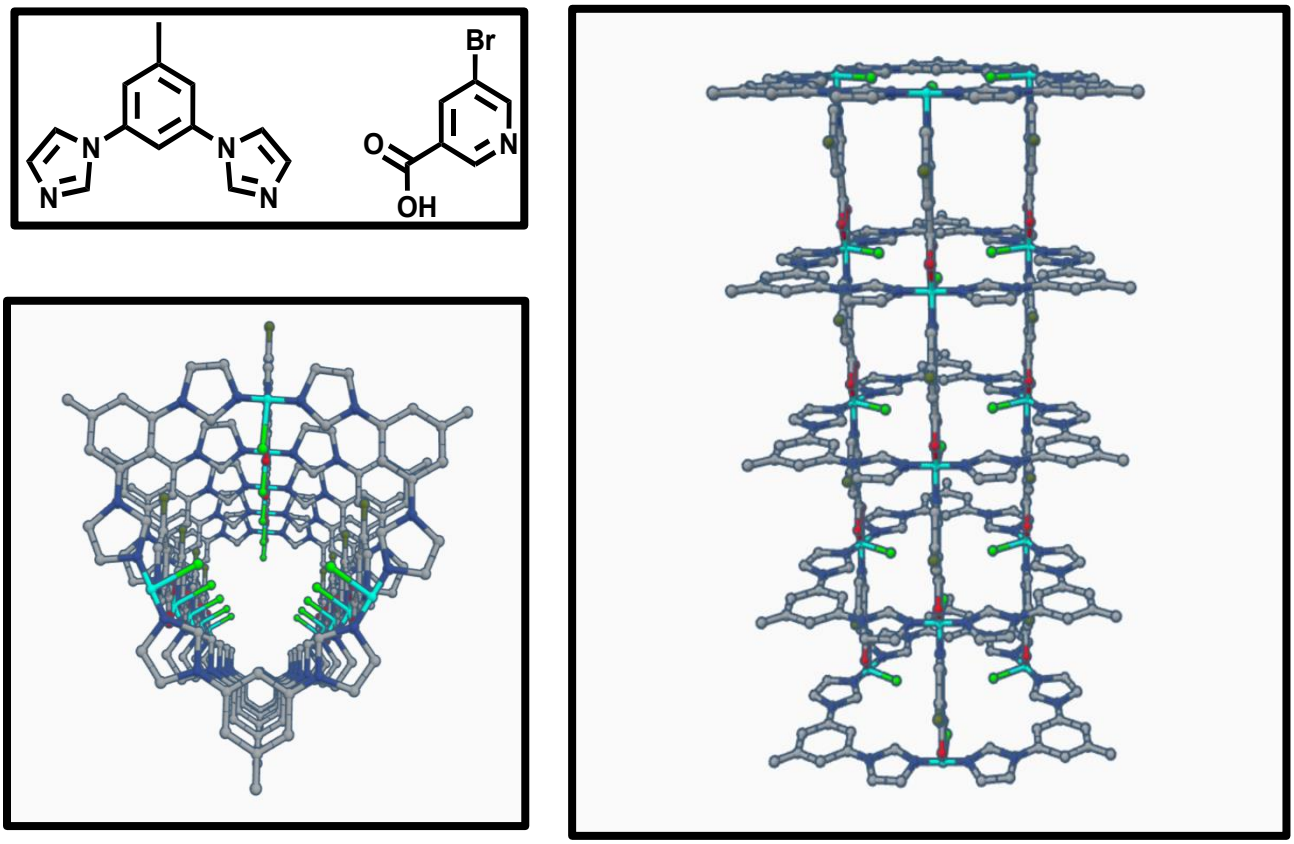

Figure 5. **(a).1,1'-(5-methyl-1,3-phenylene)bis(1H-imidazole) and 5-bromonicotinate (Brna) coordinating to a nickel center. (b). Top and (c). side facing views for the three-column pillared MONT Ni(pbim)(Brna)Cl•H_2O. MONTs synthesized by Wu and coworkers use a secondary organic linker (Brna) as both the bridging arm and "capping" agent to form the pore.**

Applying principles learned from isoreticular syntheses in literature, our research group became the first to apply these fundamentals to the construction of isoreticular MONTs.[7,13,21-22] Pioneered in 2014 by Chris Murdock, our research group developed a new category of MONT which utilized semi-ridgid di-triazole organic linkers and a group 11 metal salt to create a porous material of which height and width could be independently altered.[5,11] Highlighting this particular synthetic method, the MONTs made through this method take on a *syn* or a "c-shaped" structure of which was later generalized to the two-column pillared approach.[13] In this method of synthesis, the metal cation acts as an anchor which is half of the "building block" required for synthesis.[7,13,21-22] Interacting with the metal cation, a di-triazole binding site provides overall pore structure where finally an anionic "cap" is used to close the pore.[7,13,21-22] In the synthesis of two-pillared MONTs in our research group it is critical to note the value of the bridging arms in the di-triazole organic linkers.[7,13,21-22] These bridging arms directly influence the geometry of the formed pore and are an integral part of the two-column pillared approach (***Figure 6)***.[5]

In our research group, MONTs as a nanocrystalline material have been thoroughly analyzed with a goal of understanding and studying the anisotropic growth patterns of these one-dimensional materials (***Figure 7)***. In 2019, Kristina Vailonis used a biphenyl organic linker and through multiple trials of synthesis a group of "zipper-like" MONTs with finite growth patterns were synthesized.[7] The MONTs grown were observed in real time using liquid cell transmission electron microscopy (LCTEM) and following visualization these very same MONT materials grew for several days following analysis.[7] Once reaching the optimal size, single crystal X-ray diffraction was used in order to visualize the individual MONT tubes.[7] To

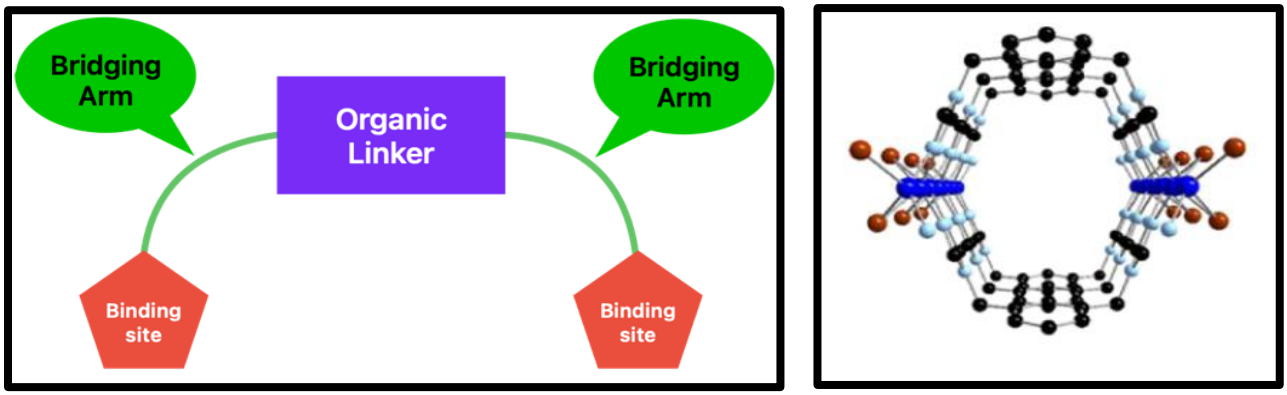

Figure 6 **(a). The structure of a di-triazole ligand is generalized (left) which represents three critical parts which shape the pore; an organic linker core (in purple), a semi-flexible bridging arm (in green), and a binding site (in red). (b). A completed MONT structure using 1,3-bis((4*H*-1,2,4-triazol-4-yl)methyl)benzene and copper (II) bromide (right). To note, the "capping" agent (in red) represents a bromide anion and is used to "close" the nanotube.**

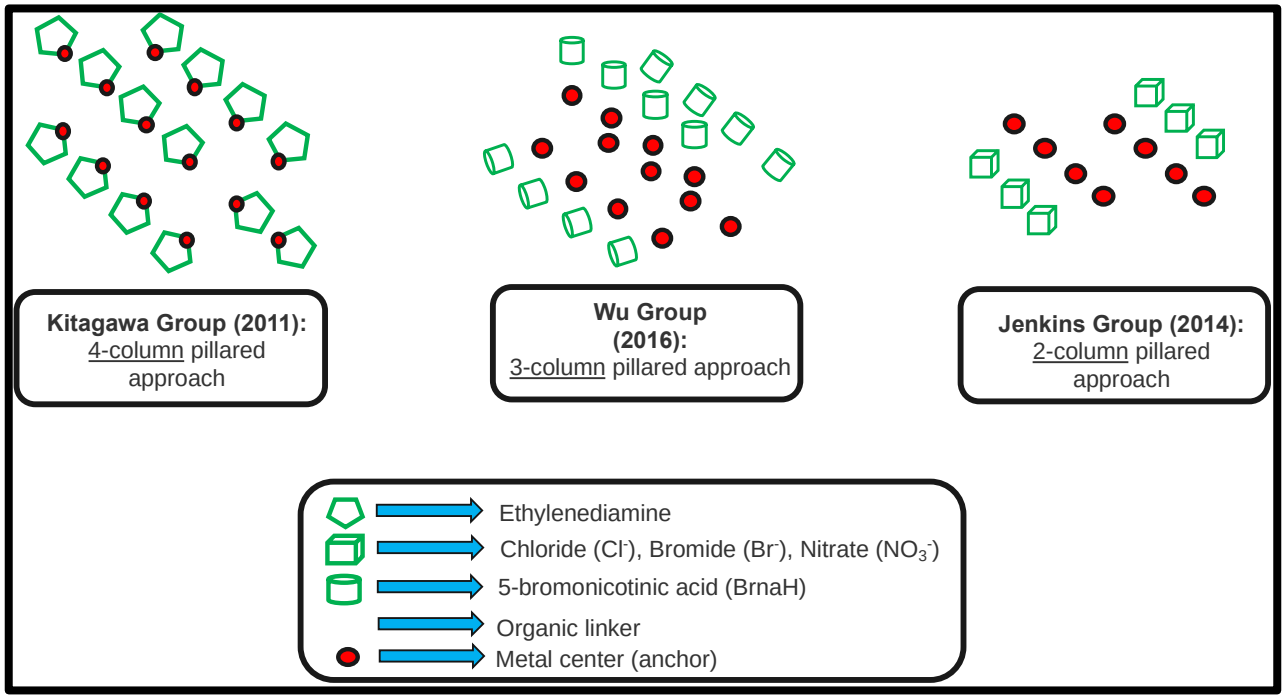

Figure 7. **Three approaches to MONT synthesis (a.) 4-column pillared, (b). three-column pillared, and (c). two-column pillared. Advantages of using the two-column pillared approach are centered on having height and width independently adjustable whereas in the four and three-column pillared approaches this is not possible due to restricted structural components.**

confirm that the nanomaterial was a match for the bulk MONT material, multiple types of instrumental analysis were implemented. Powder X-ray diffraction (PXRD), energy dispersive X-ray spectroscopy (EDS) and selected area electron diffraction (SAED) were used in order to characterize the bulk phase of the MONT which was then used to support the SCXRD data.[7] Using these different forms of instrumental analysis, it was possible to reveal elemental composition, bond-distance measuring and key diffraction patterns (***Figure 8)***.

Through methods refined by Kristina Vailonis and Chris Murdock it has been possible to characterize the new generation of MONTs which have been synthesized in recent years within our group. Building upon the work set by my predecessors, this thesis highlights the efforts of creating a MONT with pore that is much larger than any MONT synthesized prior in our group. Using methods refined by Chris Murdock and Phattananawee Nalaoh, full characterization in the form of SCXRD, PXRD, TGA and Gas Adsorption will be used as proof of concept for direct reflection on the increase of pore size in MONTs as a new innovative material. Growing the pore size of MONTs opens the door for new applications in gas storage and separations which could later lead to an expansion of future uses as a porous material.

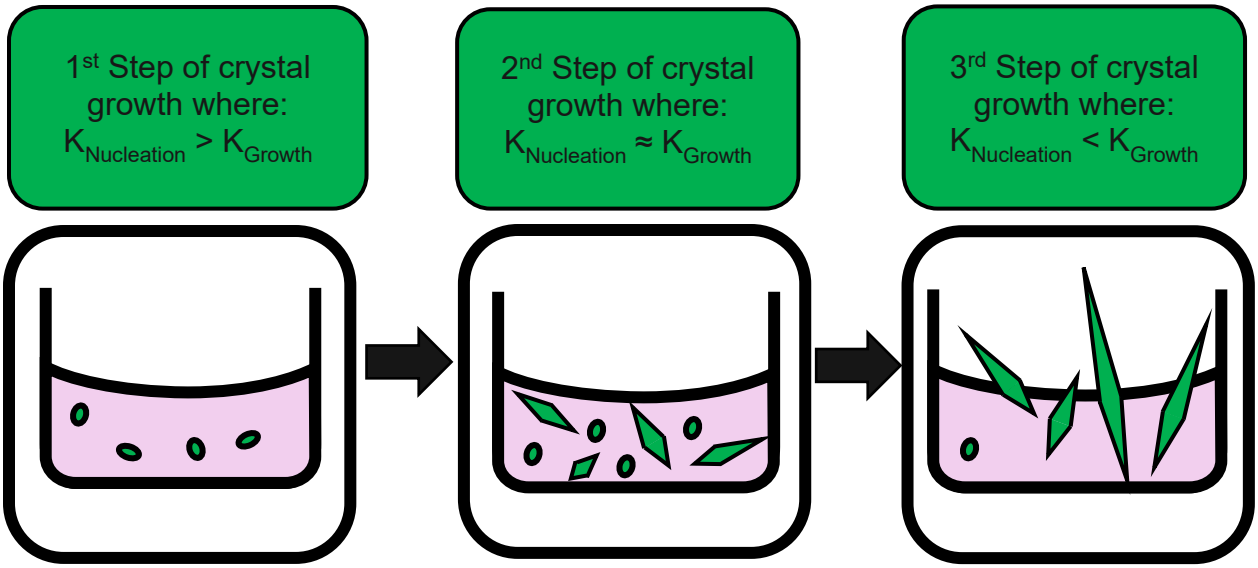

Figure 8. **Crystal growth broken into three distinct stages where in the first (left) sites of nucleation are formed, in the second (middle) nanoscale crystals begin to form, and in the third (right) microcrystals large enough for SCXRD are procured.**

References

1. Baughman, R. H.; Zakhidov, A. A.; de Heer, W. A. Carbon Nanotubes--the Route Toward Applications. *Science* **2002**, *297* (5582), 787–792.

2. Chen, D.; Tang, L.; Li, J. Graphene-based materials in electrochemistry. *Chemical Society Reviews* **2010**, *39* (8), 3157–3180.

3. Falcao, E. H. L.; Wudl, F. Carbon allotropes: beyond graphite and diamond. *Journal of Chemical Technology & Biotechnology* **2007**, *82* (6), 524–531.

4. Ferro, S. Synthesis of diamond. *Journal of Materials Chemistry* **2002**, *12* (10), 2843–2855.

5. Jia, J.-G. and Zheng, L.-M. "Metal-Organic Nanotubes: Designs, Structures and Functions" *Coordination Chemistry Reviews* 403, **2020**: 213083.

6. Otsubo, K.; Wakabayashi, Y.; Ohara, J.; Yamamoto, S.; Matsuzaki, H.; Okamoto, H.; Nitta, K.; Uruga, T.; Kitagawa, H. Bottom-up realization of a porous metal–organic nanotubular assembly. *Nature Materials* **2011**, *10*, 291–295.

7. Vailonis, K. M., Gnanasekaran, K., Powers, X. B., Gianneschi, N. C., and Jenkins, D. M. "Elucidating the Growth of Metal–Organic Nanotubes Combining Isoreticular Synthesis with Liquid-Cell Transmission Electron Microscopy" *Journal of the American Chemical Society* 141, no. 26 (**2019**): 10177–10182.

8. Furukawa, H.; Cordova, K. E.; O'Keeffe, M.; Yaghi, O. M. The Chemistry and Applications of Metal-Organic Frameworks. *Science* **2013**, *341* (6149).

9. Thanasekaran, P.; Luo, T.-T.; Lee, C.-H.; Lu, K.-L. A journey in search of single-walled metal-organic nanotubes. *Journal of Materials Chemistry* **2011**, *21* (35), 13140–13149.

10. Li, J.-R.; Ma, Y.; McCarthy, M. C.; Sculley, J.; Yu, J.; Jeong, H.-K.; Balbuena, P. B.; Zhou, H.-C. Carbon dioxide capture-related gas adsorption and separation in metal-organic frameworks. *Coordination Chemistry Reviews* **2011**, *255* (15–16), 1791-1823

11. Kuppler, R. J.; Timmons, D. J.; Fang, Q.-R.; Li, J.-R.; Makal, T. A.; Young, M. D.; Yuan, D.; Zhao, D.; Zhuang, W.; Zhou, H.-C. Potential applications of metal-organic frameworks. *Coordination Chemistry Reviews* **2009**, *253* (23–24), 3042–3066.

12. Panda, T.; Kundu, T.; Banerjee, R. Self-assembled one dimensional functionalized metal–organic nanotubes (MONTs) for proton conduction. *Chemical Communications* **2012**, *48* (44), 5464–5466.

13. Murdock, C. R.; Jenkins, D. M. Isostructural Synthesis of Porous Metal–Organic Nanotubes. *Journal of the American Chemical Society* **2014**, *136* (31), 10983–10988.

14. Adarsh, N. N.; Dîrtu, M. M.; Naik, A. D.; Léonard, A. F.; Campagnol, N.; Robeyns, K.; Snauwaert, J.; Fransaer, J.; Su, B. L.; Garcia, Y. Single-Walled Metal–Organic Nanotube Built from a Simple Synthon. *Chemistry – A European Journal* **2015**, *21* (11), 4300–4307

15. . Bu, F.; Xiao, S.-J. A 4-connected anionic metal–organic nanotube constructed from indium isophthalate. *CrystEngComm* **2010**, *12* (11), 3385–3387.

16. Kong, G.-Q.; Ou, S.; Zou, C.; Wu, C.-D. Assembly and Post-Modification of a Metal–Organic Nanotube for Highly Efficient Catalysis. *Journal of the American Chemical Society* **2012**, *134* (48), 19851–19857.

17. Fang, C.; Liu, Q.-K.; Ma, J.-P.; Dong, Y.-B. Independent 1D Nanosized Metal–Organic Tube: Anion Exchange, Separation, and Anion-Responsive Luminescence. *Inorganic Chemistry* **2012**, *51* (7), 3923–3925.

18. Qinfu, Z.; Geng, A.; Zhang, H.; Hu, F.; Lu, Z.-H.; Sun, D.; Wei, X.; Ma, C. An Independent 1D Single-Walled Metal–Organic Nanotube Transformed from a 2D Layer Exhibits Highly Selective and Reversible Sensing of Nitroaromatic Compounds. *Chemistry – A European Journal* **2014**, *20* (17), 4885–4890.

19. Jin, J.-C.; Wang, Y.-Y.; Liu, P.; Liu, R.-T.; Ren, C.; Shi, Q.-Z. An Unusual Independent 1D Metal−Organic Nanotube with Mesohelical Structure and 1D → 2D Interdigitation. *Crystal Growth & Design* **2010**, *10* (5), 2029–2032.

20. Szuromi, P. Glimpsing growing nanotubes. *Science* **2019**, *365* (6450), 246.

21. Gnanasekaran, K.; Vailonis, K. M.; Jenkins, D. M.; Gianneschi, N. C. *In Situ* Monitoring of the Seeding and Growth of Silver Metal–Organic Nanotubes by Liquid-Cell Transmission Electron Microscopy. *ACS Nano* **2020**, *14* (7), 8735–5743.

22. Nalaoh, P. and Jenkins, D. M. "Di-Triazole Boat Conformation Leads to Metal–Organic Nanotube While Chair Conformation Leads to Coordination Polymer" *CrystEngComm* 25, no. 35 (**2023**): 4929–4933.

23.Dai, F.; He, H.; Sun, D., A Metal−Organic Nanotube Exhibiting Reversible Adsorption of $(H_2O)_{12}$ Cluster. J. Am. Chem. Soc. 2008, 130, 14064-14065.

24. Li, H.; Eddaoudi, M.; O'Keeffe, M.; Yaghi, O. M.,Design and synthesis of an exceptionally stable and highly porous metal-organic framework. Nature 1999, 402, 276-279;

25. Eddaoudi, M.; Kim, J.; Rosi, N.;Vodak, D.; Wachter, J.; O'Keeffe, M.; Yaghi, O. M., Systematic Design of Pore Sizeand Functionality in Isoreticular MOFs and Their Application in Methane Storage. Science 2002, 295, 469-472.

CHAPTER 2

SYNTHESIS OF TRIAZOLES FOR EXPANSION OF METAL-ORGANIC NANOTUBE PORE SIZE

Abstract

Metal organic nanotubes (MONTs) have been synthesized under many differed approaches. With an overwhelming number of small pores synthesized, increasing the size of organic linkers used in MONT synthesis is critical to remove the size restrictions. The studies discussed in this chapter revolve around investigating how an increase in organic linker size can influence the size of a subsequent grown MONT.

Introduction

Determined by its dimensionality, the properties and applications of a material can be altered. Intentionally adjusting the pore height or pore width using various synthetic methods is integral to the development of MONTs that can take on desirable attributes for gas storage and adsorption, catalysis, liquid phase extractions and post-synthetic external site modification. As pore size increases in any material, the size of guest molecules that can be introduced to the pore can also directly increase as well.

When thinking of a porous material with many applications, most will immediately think of the multidimensional counterpart to MONTs, which are MOFs. In reviewing Metal-organic frameworks (MOFs), this material is well known for its uses in heterogenous catalysis, gas separations and storage.[4,9,10] However, the properties of this class of material are dictated by two pieces, an organic and an inorganic component. In order to properly evaluate the applications of this class of material, a selection occurs where an ideal organic linker is selected which directly influences the size of the formed pore.[1-8] Ohmar Yaghi and coworkers stressed the significance of MOFs as a material in the year 2013.[4,9,10] In this published review, many different avenues of research were reviewed and discussed with the primary four being, pore size increase for the inclusion of non-gaseous molecules, acting as a supporting agent in

catalysis, applications using gas adsorption to develop a new way to carry fuel, and applications using separations in order for cleaner air.[4,9,10] Currently, MONTs have size restrictions of which is a primary limiting agent for their applications as a material.[18-21] However, as MONTs are effectively a form of 1-dimensional MOF, our research group aims to mitigate these limitations by synthesizing MONTs with an increased pore size.[3,7]

Pioneered by Chris Murdock, isoreticular MONTs were synthesized using silver(I) nitrate and a short selection of organic di-triazole linkers.[7] Focusing primarily on the use of phenyl and napthl-based linkers, the synthesized MONT had shown that when increasing the size of the organic di-triazole linker a growth of pore could be visualized.[7] (***Figure 9)*** Placing an emphasis on one half of the synthetic puzzle, the synthesis of di-triazole organic linkers have generally followed a similar chemical process. Starting with a dibrominated precursor, this organic ligand undergoes an S_N2 substitution reaction to form a protected di-triazole organic linker which then undergoes an E2 elimination forming the final desired di-triazole organic linker.[7,22] ***(Figure 10)***

Utilizing concepts and techniques outlined by previous group members, a series of organic linkers were designed with the purpose of testing the limits of pore expansion for MONT synthesis. Shown in ***Figure 13***, this select series of organic linkers were hypothesized to generate a larger MONT pore when compared to that of previously published results. Herein this chapter, the investigation that took place focused on the synthesis of these expanded organic linkers, their characterization, and their differences.

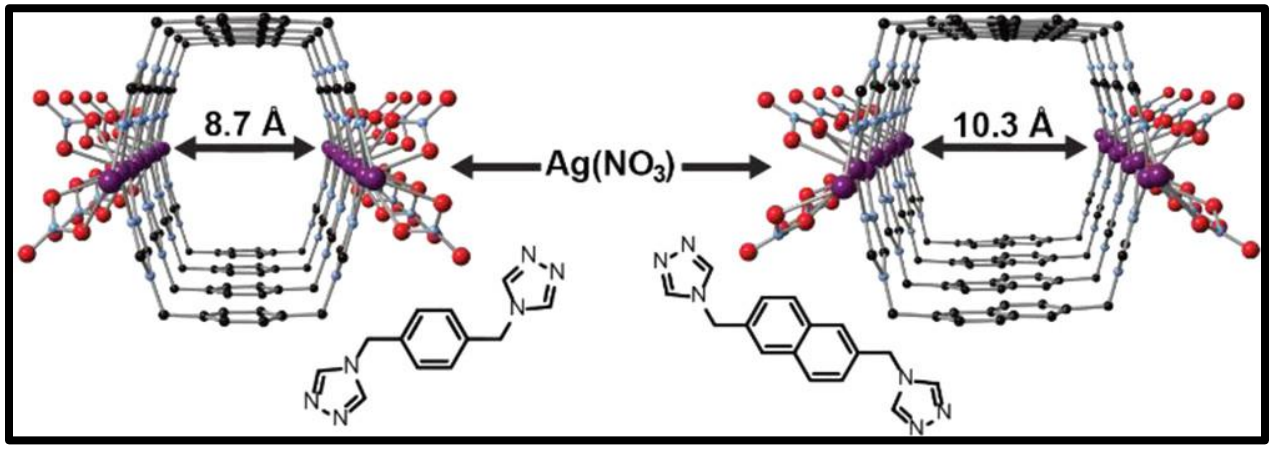

Figure 9. **Two silver MONTs shown using Single Crystal X-Ray Diffraction (SCXRD) which show that as the size of the organic linker increases in width, the size of the MONT pore also reflects this change.**

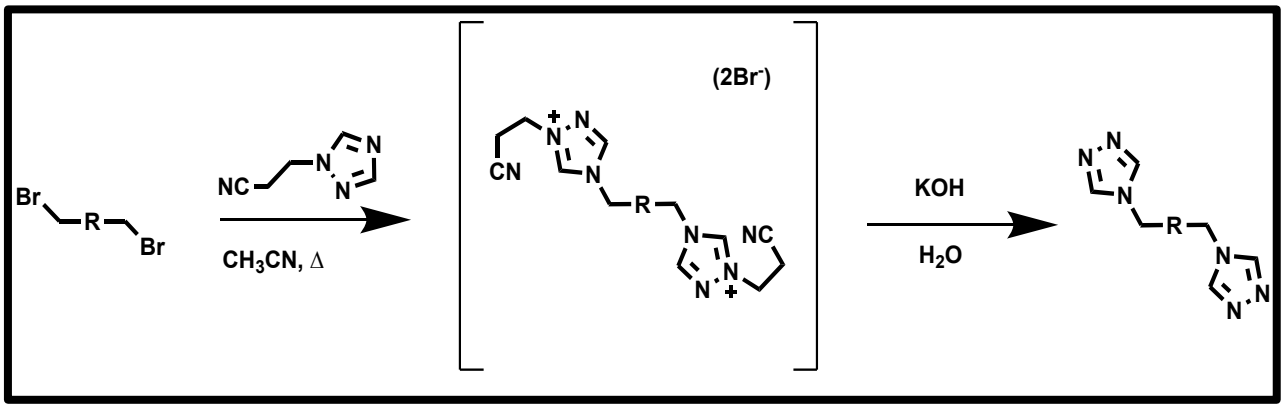

Figure 10. **Synthetic scheme followed for the synthesis of di-triazole type organic linkers which was refined by Dr. Chris Murdock and coworkers.**

Results and Discussion

When conducting research on this relatively new class of material, the phrase "dimensionality dictates function" has stood strong as the primary building block towards the formed hypothesizes and discoveries herein this chapter. To highlight an important definition, isoreticularity can be defined as one material having a similar topology when compared to that of another material.[4,9,10] Omar Yaghi pioneered the development of these isoreticular MOFs of which despite selecting a myriad of organic linkers for synthesis, the underlying topology remained the same.[4,9,10] Keeping these principles in mind, a series of syn-conforming organic linkers were selected that would result in the same underlying topology as the previously synthesized MONTs while also increasing the overall pore size.[3,7,22]

Shown in ***Figure 10***, Chris Murdock refined the original method of Horváth and in doing so created a template which has been an integral part to the development of new organic linkers.[7] Beginning with one of the pioneering isostructural MONT synthesis reactions, 1,3-bis((4*H*-1,2,4-triazol-4-yl)methyl)benzene can be synthesized with a high purity when starting from pure 1,3-bis(bromomethyl)benzene.[7] Using 1,3-bis(bromomethyl)benzene and reacting it with 3-(1H-1,2,4-triazol-1-yl)propanenitrile in a solution of acetonitrile at reflux results in the synthesis of the protected precursor ligand. This 4,4'-(1,3-phenylenebis(methylene))bis(1-(2-cyanoethyl)-4*H*-1,2,4-triazol-1-ium) then undergoes an elimination reaction using either potassium hydroxide or ammonium hydroxide to form the final purified 1,3-bis((4*H*-1,2,4-triazol-4-yl)methyl)benzene product.[7] Under these particular reaction conditions, it has been possible to synthesize a series of organic linkers that accomplish the goal of developing ligands for future pore expansion.[3,7,22] Highlighting key characteristics of the 2-column pillared

approach, using various different styles of organic linkers it can be hypothesized that the height and the width of a synthesized MONT can be altered.

Shown in ***Figure 11,*** one particular organic linker was synthesized which was predicted to adjust the height of MONTs developed. The starting material 4,4''-bis(bromomethyl)-1,1':3',1''-terphenyl (**1a)** was refluxed in acetonitrile with 3-(1H-1,2,4-triazol-1-yl)propanenitrile (**1b**) to form 4,4'-([1,1':3',1''-terphenyl]-4,4''-diylbis(methylene))bis(1-(2-cyanoethyl)-4*H*-1,2,4-triazol-1-ium) (**1c)** This product then underwent an E2 elimination reaction using ammonium hydroxide in order to from the final product of 4,4''-bis((4*H*-1,2,4-triazol-4-yl)methyl)-1,1':3',1''-terphenyl (**1d**). Once this reaction had reached completion (**1d)**, two separations were required in order to extract the desired final product. Within this reaction mixture there was one main issues that had arisen, due to the bulky size of this organic linker finding a solvent where it was completely miscible had proven to be rather difficult. To combat this, two separations had taken place where the first separation occurred in dichloromethane. The desired product that was trapped within an undesired byproduct of acrylonitrile was slowly dissolved by stirring at 40°C. Once the dichloromethane had evaporated, more dichloromethane was added and then following this a second extraction in ethyl acetate took place. Completion of this second extraction yielded a off-white oil where diethyl ether was then added which caused a bright white precipitate to form. After drying the product on a Schlenk line, bright white needles could be visualized which were then used for both NMR and SCXRD analysis. Represented by the complete assignment in ***Figure 12,*** three different types of NMR were employed (^{1}H, ^{13}C and HSQC) in order to fully characterize this expanded organic linker. For further supporting evidence, a large white needle obtained from the pure product was ran using SCXRD showing a complete visual of the expanded organic linker.

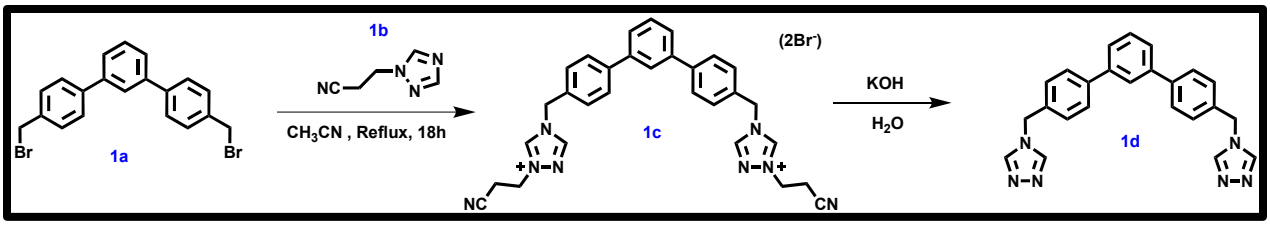

Figure 11. **Synthetic scheme adapted from the method of Horváth for the synthesis of 4,4''bis((4*H*-1,2,4-triazol-4-yl)methyl)-1,1':3',1''-terphenyl.**

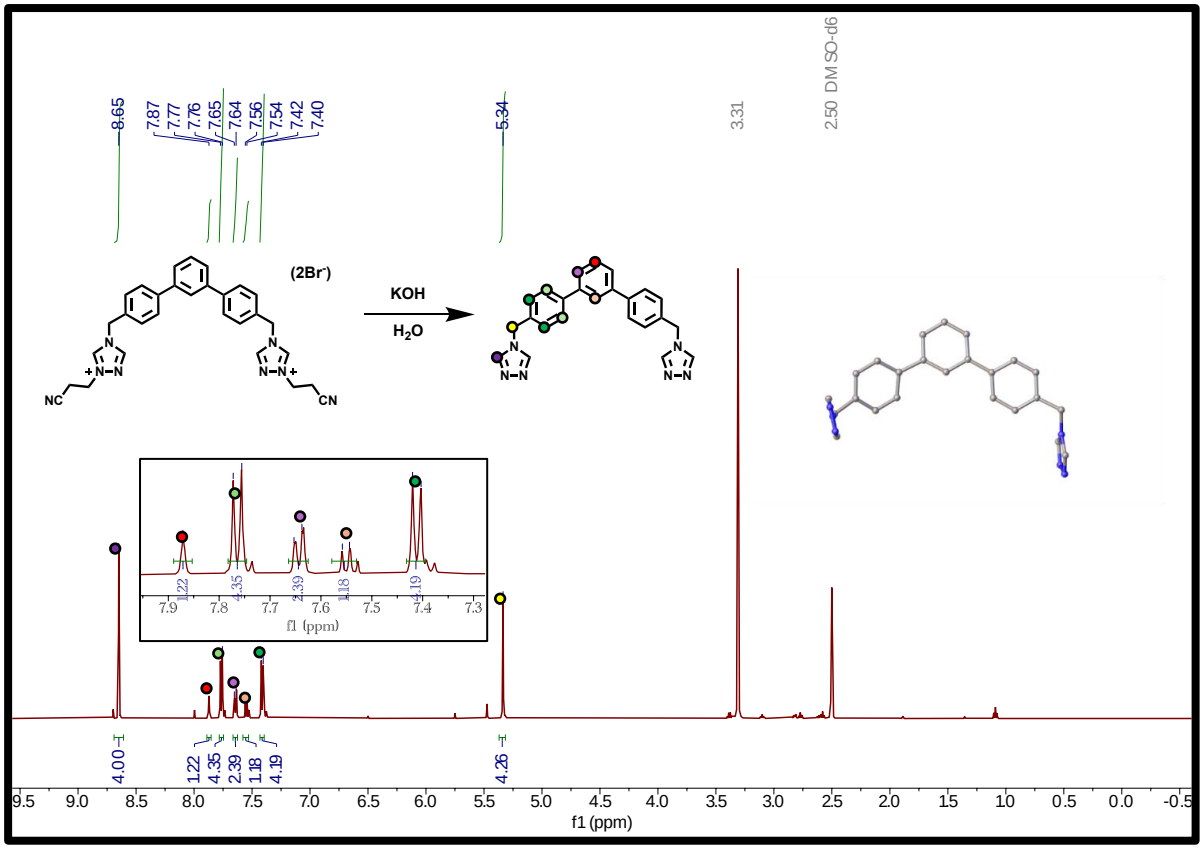

Figure 12. **NMR and SCXRD analysis of 4,4''-bis((4*H*-1,2,4-triazol-4-yl)methyl)-1,1':3',1''-terphenyl where each unique signal is labelled with a different color. The aromatic region is enlarged for easier viewing and the hydrogens are omitted on the SCXRD for further clarity. To note, N is blue and C is grey on SCXRD.**

With a confirmed and completed organic linker (**1d**) that was engineered specifically to adjust height, looking at a series of organic linkers that would adjust width was deeply investigated. Represented in ***Figure 13*** is a series of large organic linkers of which were predicted to have various widening effects on the structure of MONTs. Many of the following organic linkers (**2a-4c)** yielded various levels of either success or complications along the synthetic pathways. One such linker, which was selected for its freedom of rotation was bis(4-((4*H*-1,2,4-triazol-4-yl)methyl)phenyl)methane which was synthesized starting at a bis(4-(bromomethyl)phenyl)methane (**2a**) precursor. This solid white powder is refluxed in acetonitrile with 3-(1H-1,2,4-triazol-1-yl)propanenitrile which yields the pure product 4,4'-((methylenebis(4,1-phenylene))bis(methylene))bis(1-(2-cyanoethyl)-4*H*-1,2,4-triazol-1-ium). Upon drying under vacuum this white powder was then added to a solution of potassium hydroxide where it was set to stir for 24 hours under reflux. A cloudy solution was observed after completion and a separation in ethyl acetate took place resulting in a clear organic phase and a white aqueous phase. The organic phase was then dried under vacuum resulting in an off white oil. This off white oil was then covered in a layer of 50/50 isopropyl alcohol and diethyl ether before being placed in a freezer which upon cooling overnight resulted in a bright white precipitate. The following pure bis(4-((4*H*-1,2,4-triazol-4-yl)methyl)phenyl)methane was then placed under vacuum to dry before characterization.

Two more organic linkers were developed with pore width expansion in mind, these two being 1,2-bis(4-((4*H*-1,2,4-triazol-4-yl)methyl)phenyl)ethyne (**3c)** and 2,7-bis((4*H*-1,2,4-triazol-4-yl)methyl)phenanthrene (**4c)**. The thought behind the development of organic linker **3c** was the presence of the alkyne bridge which was predicted to cause the linker to be locked in a flat plane

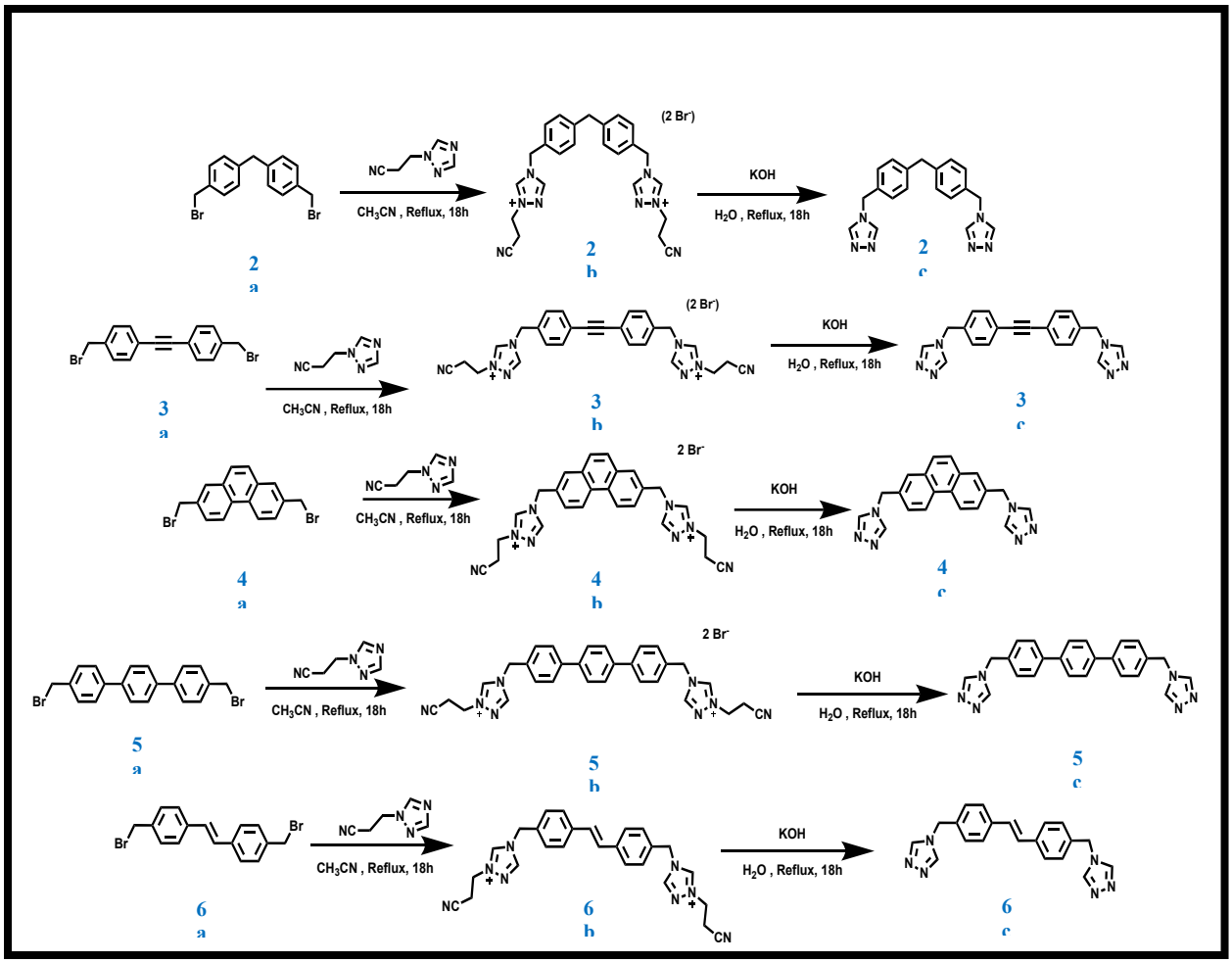

Figure 13. **Expanding on preliminary results for pore expansion (1d), many other organic linkers and their precursors (3a-4c) were synthesized in order to achieve an understanding of the broad-scale impacts an organic linker has on the potential of MONT formation. To further expand the number of organic linkers available in the MONT library, precursors and organic linkers (5a-6c) were planned for future reactions to determine success or failure.**

with minimal movement about the carbon-carbon triple bond. Following the same chemical workup as discussed for ligand **1d,** the synthesis of **3c** had the same temperament where it was incredibly hygroscopic in water and partially miscible in both dichloromethane and ethyl acetate. The final product was a small off-yellow crystalline material which when left at room temperature would transition from a solid to an oil. In order to maintain the integrity of the 1,2-bis(4-((4*H*-1,2,4-triazol-4-yl)methyl)phenyl)ethyne organic linker, it was first flushed with nitrogen before being stored in a freezer. ***Figure 14*** shows a stacked ^{1}H-NMR of organic linker **3c** and two precursors **3a** and **3b,** this has significance as a peak shown at approximately 3.3ppm is indicative of water. To clarify, as this ligand reaches completion, the amount of water retained also dramatically increases. ***Figure 15*** sparks an interesting conversation in which optimization is a key component. The following figure is a series of ^{1}H-NMR depicting various different complications surrounding ligand synthesis for this 2,7-bis((4*H*-1,2,4-triazol-4-yl)methyl)phenanthrene organic linker. 2,7-bis(bromomethyl)-9,10-dihydrophenanthrene was added to a solution of benzene and 2,3-Dichloro-5,6-dicyano-1,4-benzoquinone before refluxing for 24 hours. After workup, the resulting product was a very light, fluffy white powder which had a bulky appearance but a very low mass when weighed. The resulting 2,7-bis(bromomethyl)phenanthrene was then dissolved in a solution of acetonitrile and 3-(1H-1,2,4-triazol-1-yl)propanenitrile before bringing up to reflux temperature and reacting overnight. After completion of this reaction, the wet product was dried under vacuum and a porous off-white material was obtained. The resulting 4,4'-(phenanthrene-2,7-diylbis(methylene))bis(1-(2-cyanoethyl)-4*H*-1,2,4-triazol-1-ium) was analyzed using NMR and a minor undesired byproduct was detected in the 9.5 to 10.5 ppm region.

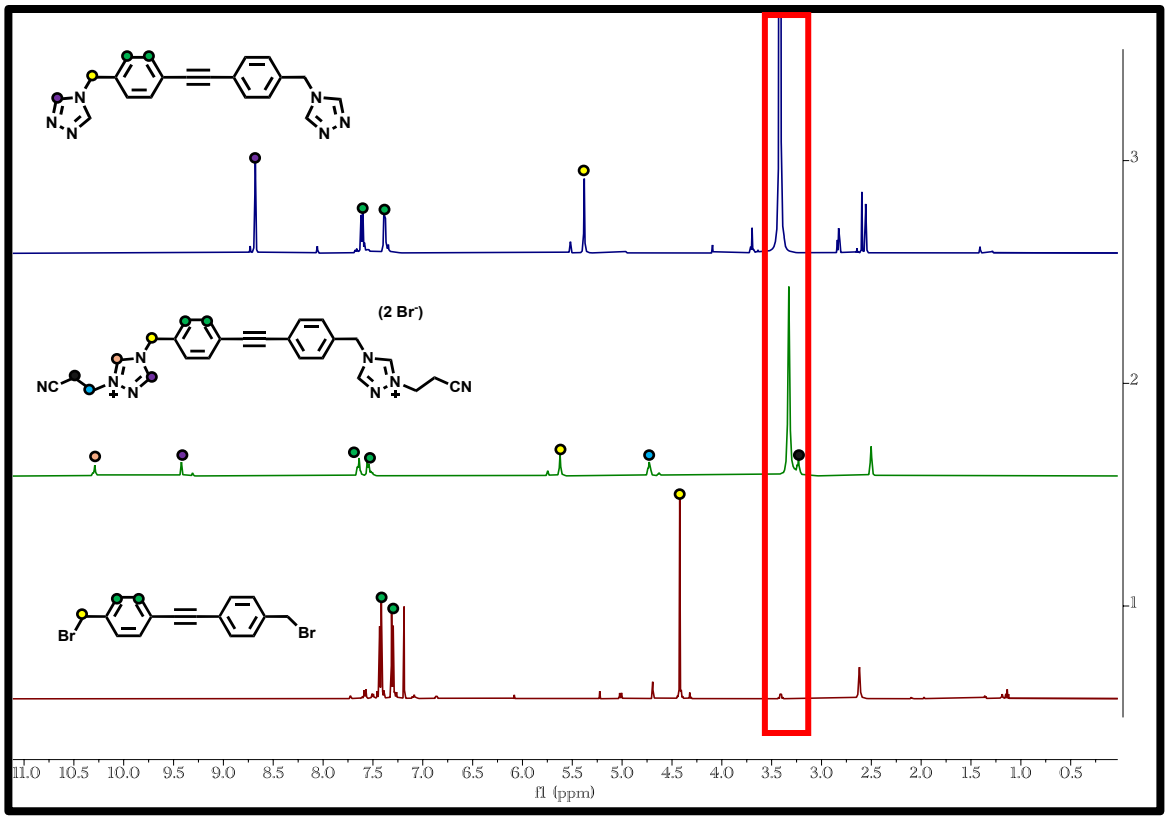

Figure 14. **^{1}H-NMR analysis of 1,2-bis(4-(bromomethyl)phenyl)ethyne (3a), 4,4'-((ethyne-1,2-diylbis(4,1-phenylene))bis(methylene))bis(1-(2-cyanoethyl)-4*H*-1,2,4-triazol-1-ium) (3b), and 1,2-bis(4-((4*H*-1,2,4-triazol-4-yl)methyl)phenyl)ethyne (3c). The above ^{1}H-NMR spectrum show a clear trend in water-sensitivity which increased throughout each synthetic step.**

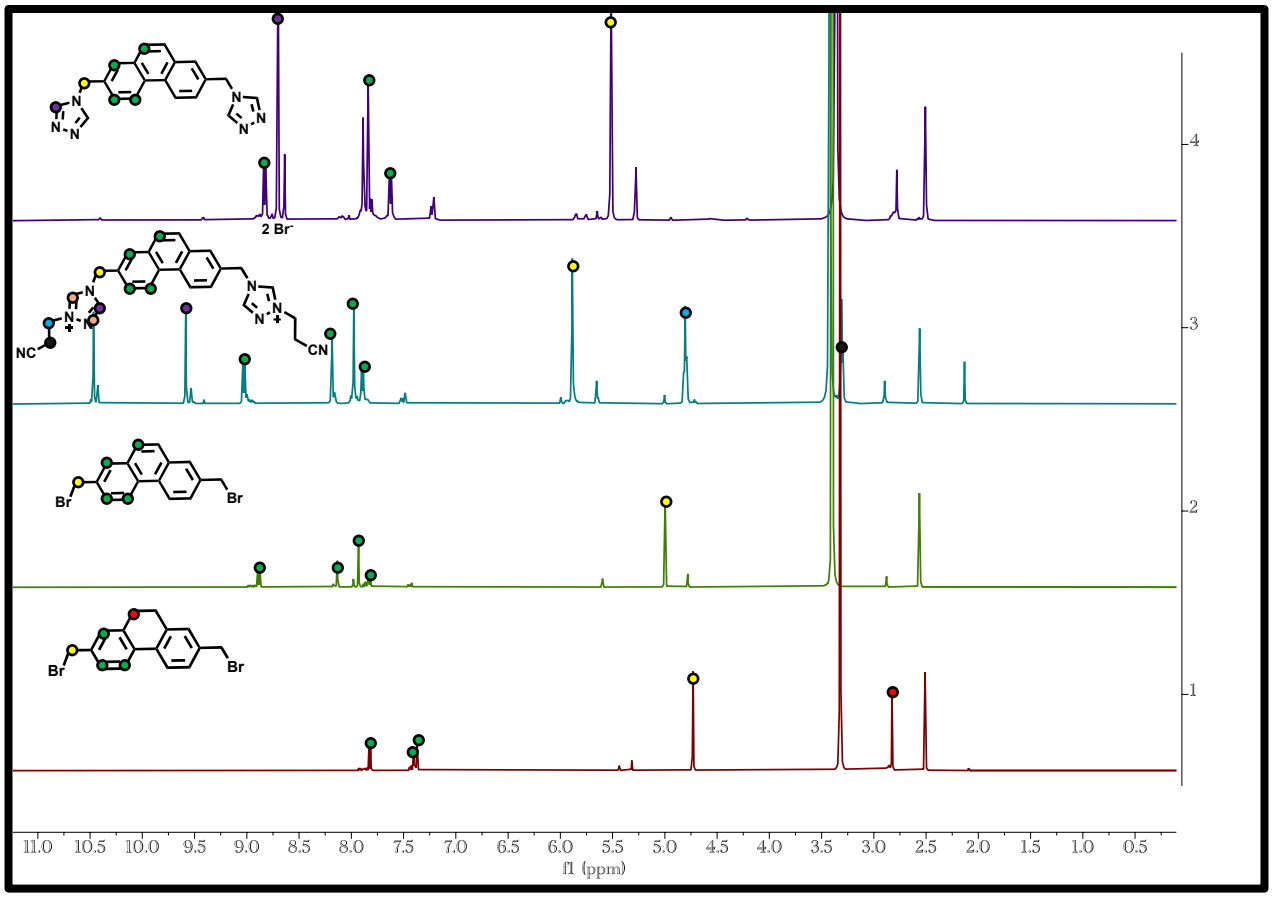

Figure 15. **^{1}H-NMR analysis of 2,7-bis(bromomethyl)-9,10-dihydrophenanthrene, 2,7-bis(bromomethyl)phenanthrene, 4,4'-(phenanthrene-2,7-diylbis(methylene))bis(1-(2-cyanoethyl)-4*H*-1,2,4-triazol-1-ium), and 2,7-bis((4*H*-1,2,4-triazol-4 yl)methyl)phenanthrene. The above ^{1}H-NMR spectrum shows isomerization occurring where in the final step of synthesis there is the desired major di-substituted (labeled) and trace amounts of two predicted undesired mono-substituted products (unlabeled). This organic linker is extremely hygroscopic and retains water at each step of synthesis.**

After careful review this predicted byproduct was determined to have been a result of minor impurities in the 3-(1H-1,2,4-triazol-1- yl) propanenitrile which can form two different isomers resulting in slightly different ppm values on NMR. Due to complexities surrounding salt purification, this impure organic precursor was used for the synthesis of the 2,7-bis((4*H*-1,2,4-triazol-4-yl)methyl)phenanthrene ligand with hopes of purification occurring post-synthesis. Reacting the impure 4,4'-(phenanthrene-2,7-diylbis(methylene))bis(1-(2-cyanoethyl)-4*H*-1,2,4-triazol-1-ium) with potassium hydroxide under reflux for 24 hours resulted in a solution with two layers, one of which was cloudy and the other was viscous and brown. This solution underwent two different separations, the first taking place in dichloromethane where the solution was rinsed until the brown layer and cloudy layer became a miscible yellow solution with clear distinctions between the potassium hydroxide layer and the dichloromethane layer. This dichloromethane organic phase was dried under vacuum resulting in an oily yellow product. Dichloromethane was added back to this oil and ethyl acetate was also added to perform the second separation. After this second separation took place, the ethyl acetate layer was dried under vacuum resulting in a white sticky paste. Isopropyl alcohol, diethyl ether and ethanol was added to this paste, swirled and set in the freezer overnight. Upon removal the next day, a white precipitate had formed in solution and the solution was decanted off the solid precipitate. The precipitate was then dried under vacuum resulting in a dense, porous, white powder. Once NMR analysis was completed, it was determined that two undesired byproducts had remained, one of which the very first precursor 2,7-bis(bromomethyl)-9,10-dihydrophenanthrene, and the other being an unknown product which was speculated to being a retained minor isomer. The organic linker 2,7-bis((4*H*-1,2,4-triazol-4-yl)methyl)phenanthrene

was not easily purified due to issues with being extremely hygroscopic and having poor miscibility with many organic solvents.

Conclusions

The synthesis of MONTs begins with the selection of an organic linker that will provide both repeatable and novel results. When reviewing literature there have been numerous MONTs synthesized with a restricted pore size which also restricts its use in the advancement of MONTs as a porous material. In order to accomplish the goal of pore expansion, many organic linkers need to be synthesized which are later used in the analysis of both confirmed and unknown MONT growth. In this chapter three organic ligands were completely purified and used for testing of MONTs (**1a-3c**), one organic linker was synthesized but not considered complete due to purification issues (**4a-4c)** and two other organic linkers (**5a-6c)** had schemes written and planned, but due to issues with solubility, purification, and cost did not leave the preliminary stages of development. Alternate routes for synthesis of precursors are currently being reviewed in order to overcome the issues listed prior, and upon the completion of these adjustments it could be possible to develop pure, simple, and effective chemical reactions based on literature classics. Although the work in this chapter did not result in a completed expansion of the organic library for pore enlargement, it has proven to become the foundation and starting point for the development of future organic linkers.

Experimental

Synthesis of [1,1':3',1''-terphenyl]-4,4''-diyldimethanol: [1,1':3',1"-terphenyl]-4,4"-diyldimethanol (precursor to **1a**) was prepared in bulk according to previously reported procedures.[11] 30.00 g (127.2 mmol) of 1,3-dibromobenzene, 42.91 g (282.4 mmol) of 4-(hydroxymethyl)benzylboronic acid, 7.411 g (6.414 mmol)

tetrakis(triphenylphosphine)palladium(0), 100 mL of 2 M sodium carbonate solution in water, and 300 mL of tetrahydrofuran were combined in a clean, dry 1000 mL round bottom flask and refluxed under N_2 for 48 hours. The reaction was then cooled to room temperature before being rinsed with 100 mL of brine and extracted using 200 mL of dichloromethane. The organic layer was then dried using magnesium sulfate and filtered, concentrated under reduced pressure and 150 mL of methanol was added in order to perform a recrystallization. The reaction flask was then placed in a -20 °C freezer overnight and upon removal the next morning, bright white crystals were visualized in solution. This solution was then poured over a frit, dried using vacuum filtration, and the bright white crystals were rinsed with ~30 mL of cold methanol before drying a second time under reduced pressure using a Schlenk line. (30.04g, 81.3% yield). ^{1}H-NMR (DMSO-d_6, 499.74 MHz): σ 7.88 (t, J = 7.8 Hz, 1H), 7.72 (d, J = 7.7 Hz, 4H), 7.63 (d, J = 7.6 Hz , 2H), 7.54 (t, J = 7.5 Hz ,1H), 7.43 (d, J = 7.4 Hz, 4H), 5.22 (t, J = 5.2 Hz, 2H), 4.56 (d, J = 4.6 Hz, 4H). ^{13}C{^{1}H} NMR (DMSO-d_6, 125.67 MHz): σ 141.94, 140.78, 138.52, 129.49, 127.00, 126.59, 125.52, 124.82, 62.61. IR: 3265, 2917, 2850, 1472, 1434, 1389, 1185, 1093, 996, 855, 791, 771, 718, 691, 602, 560 cm^{-1}.

Synthesis of 4,4''-bis(bromomethyl)-1,1':3',1''-terphenyl (1a): (**1a**) was prepared in bulk according to previously reported procedures. [12] 5.00 g (17.2 mmol) of [1,1':3',1"-terphenyl]-4,4"-diyldimethanol, 10.00 mL (105.3 mmol) of phosphorus tribromide, and 100 mL of dichloromethane were combined in a clean, dry 250 mL round bottom flask, cooled in a methanol/ice bath, and stirred under N_2 for 48 hours. Upon completion, this reaction was quenched with 200 mL of ice water and extracted with 200 mL of dichloromethane. The organic phase was dried with magnesium sulfate, concentrated, and the product was precipitated with 150 mL of diethyl ether as thin white needles (4.67 g , 65.2% yield). ^{1}H-NMR (DMSO-d_6,

499.74 MHz): σ 7.84 (t, J = 7.8 Hz , 1H), 7.68 (d, J = 7.7 Hz ,4H), 7.59 (d, J = 7.6 Hz , 2H), 7.47 (d, J= 7.5 Hz 4H), 4.70 (s, 4H). $^{13}C\{^{1}H\}$ NMR (DMSO-d_6, 125.67 MHz): σ 140.25, 139.97, 137.36, 129.87, 129.59, 127.20, 126.04, 125.14, 34.29. IR: 3033, 2864, 1601, 1515, 1476, 1436, 1390, 1226, 1205, 1104, 840, 788, 766, 734, 695, 602, 585 cm^{-1}.

Synthesis of 3-(1H-1,2,4-triazol-1-yl)propanenitrile (1b): The following compound was synthesized as previously reported.[7]

Synthesis of 4,4'-([1,1':3',1''-terphenyl]-4,4''-diylbis(methylene))bis(1-(2-cyanoethyl)-4*H*-1,2,4-triazol-1-ium)dibromide (1c): 3.00 g (7.21 mmol) of 4,4"-bis(bromomethyl)-1,1':3',1"-terphenyl, 1.80 g (14.4 mmol) of 3-(1H-1,2,4-triazol-1-yl)propanenitrile, and 100 mL of acetonitrile were combined in a clean, dry 250 mL round bottom flask and brought to reflux for 18 hours. Upon completion, a white precipitate formed. The solids were removed via filtration, washed with 30 mL of acetonitrile 3 times, and dried under vacuum to yield a white fluffy powder. (4.623 g, 97.0% yield) ^{1}H-NMR (DMSO-d_6, 499.74 MHz): σ 10.41 (s, 2H), 9.52 (s, 2H), 7.93 (t, J = 7.9 Hz , 1H), 7.87 (d, J = 7.8 Hz , 4H), 7.71 (d, J = 7.7 Hz , 2H), 7.65 (d, J = 7.6 Hz, 4H), 7.61 (d, J = 7.6 Hz , 1H), 5.67 (s, 4H), 4.75 (t, J = 4.8 Hz , 4H), 3.35 (t, J = 3.3 Hz , 4H). $^{13}C\{^{1}H\}$ NMR (DMSO-d_6, 125.67 MHz): σ 145.50, 143.89, 141.20, 140.60, 133.30, 130.01, 128.06, 126.80, 125.70, 118.20, 50.78, 47.76, 17.81. IR: 3010, 2250, 2162, 1980, 1577, 1344, 1206, 1064, 915, 829, 785, 756, 732, 716, 687, 675, 603, 562, 554 cm^{-1}.

Synthesis of 4,4''-bis((4*H*-1,2,4-triazol-4-yl)methyl)-1,1':3',1''-terphenyl (1d): 6.00 g (9.08 mmol) of 4,4'-([1,1':3',1"-terphenyl]-4,4"-diylbis(methylene))bis(1-(2-cyanoethyl)-4*H*-1,2,4-triazol-1-ium dibromide) was suspended in 150 mL of a 6M solution of potassium hydroxide in water at reflux in a clean, dry, 250 mL round bottom flask overnight. Once the reaction reached completion, two separate extractions took place. 200 mL of dichloromethane was added to the

150 mL potassium hydroxide solution and transferred to a separatory funnel for the first extraction. After three rinses with an additional 30 mL of dichloromethane, this organic layer was separated and concentrated under reduced pressure resulting in a crude oil. To the aqueous layer, 200 mL of ethyl acetate was added. The aqueous layer was then rinsed twice with an additional 2x25 mL of ethyl acetate. The organic ethyl acetate layer was then separated and dried under reduced pressure resulting in a crude oil. The two separate fractions of crude oil were then both redissolved in 150 mL of ethyl acetate, mixed, and dried over magnesium sulfate. This final organic layer was then concentrated, and a final purified product was precipitated out as a white powder using 50 mL of diethyl ether. (2.78 g , 78.0% yield) ^{1}H-NMR (DMSO-d_6, 499.74 MHz): σ 8.65 (s, 4H), 7.87 (t, J = 7.9 Hz ,1H), 7.76 (d, J = 7.7 Hz , 4H), 7.64 (d, J = 7.6 Hz , 2H), 7.54 (t, J = 7.5 Hz, 1H), 7.41 (d, J = 7.4 Hz , 4H). ^{13}C{^{1}H} NMR (DMSO-d_6, 125.67 MHz): σ 143.27, 140.29, 139.82, 136.04, 129.58, 128.29, 127.38, 126.00, 125.17, 47.23. IR: 3108, 2938, 1668, 1530, 1445, 1376, 1175, 1073, 857, 798, 775, 752, 701, 630, 540 cm^{-1}.

Synthesis of bis(4-(bromomethyl)phenyl)methane (2a): Bis(4-(bromomethyl)phenyl)methane (**2a**) was prepared in bulk according to previously reported procedures. [13] To a clean, dry, 500 mL round bottom flask, 24.00 g (142.6 mmol) of diphenylmethane and 18.0 g (600 mmol) of paraformaldehyde were added to approximately 50 mL of 33% HBr in glacial acetic acid. This reaction was then brought to reflux at 100 °C where it was stirred for 13 hours. After completion the reaction was immersed in an ice bath, washed with cold DI water and recrystallized from approximately 30mL of diethyl ether. To note, small white crystals formed and could be seen under a microscope. (18.32g, 36.0% yield). ^{1}H-NMR ($CDCl_3$, 499.74 MHz): σ 7.32 (d, J = 7.3 Hz , 4H), 7.16 (d, J = 7.2 Hz , 4H), 4.48 (s, 4H), 3.97 (s, 2H). ^{13}C{^{1}H} NMR ($CDCl_3$, 125.67

MHz): σ 141.10, 135.78, 129.37, 129.29, 41.34, 33.48. IR: 3046, 1512, 1432, 1416, 1225, 1197, 1177, 1095, 1021, 863, 846, 823, 794, 764, 714, 627, 595, 583, 560 cm^{-1}.

Synthesis of 4,4'-((methylenebis(4,1-phenylene))bis(methylene))bis(1-(2-cyanoethyl)-4*H*-1,2,4-triazol-1-ium) dibromide (2b): 15.00 g (42.36 mmol) of bis(4-(bromomethyl)phenyl)methane, 11.38 g (93.19 mmol) of 3-(1H-1,2,4-triazol-1-yl)propanenitrile, and 150 mL of acetonitrile were combined in a clean, dry, 500 mL round bottom flask and refluxed for 18 hours. Upon completion, a white precipitate formed. The solids were removed via filtration, washed with 30 mL of acetonitrile 3 times, and dried under vacuum to yield a white fluffy powder. (13.42 g, 53.0% yield) ^{1}H-NMR (DMSO-d_6, 499.74 MHz): σ 10.34 (s, 2H), 9.43 (s, 2H), 7.43 (d, J = 7.4 Hz , 4H), 7.32 (d, J = 7.3 Hz , 4H), 5.54 (s, 4H), 4.71 (t, J = 4.7 Hz , 4H), 3.97 (s, 2H), 3.22 (t, J = 3.2 Hz , 4H). ^{13}C{^{1}H} NMR (DMSO-d_6, 125.67 MHz): σ 145.41, 143.77, 142.48, 131.78, 129.82, 129.51, 118.18, 50.77, 47.72, 17.78. IR: 3029, 2254, 1583, 1511, 1440, 1143, 1069, 1023, 853, 827, 753, 641, 615, 597, 580, 559 cm^{-1}.

Synthesis of bis(4-((4*H*-1,2,4-triazol-4-yl)methyl)phenyl)methane (2c): To a clean, dry, 250 mL round bottom flask, 2.00 g (3.34 mmol) of 4,4'-((methylenebis(4,1-phenylene))bis(methylene))bis(1-(2-cyanoethyl)-4*H*-1,2,4-triazol-1-ium) dibromide was suspended in 100 mL of a 6M solution of potassium hydroxide in water at reflux in a clean, dry, 250 mL round bottom flask overnight. The resulting suspension was separated with 100 mL of ethyl acetate, resulting in a clear organic phase and a white aqueous phase. The organic phase was then dried under vacuum resulting in an off-white oil. This oil was then covered in a layer of 100 mL of 50/50 isopropyl alcohol and diethyl ether, placed in a freezer, and after cooling overnight yielded a bright white precipitate. (880 mg, 80.0% yield) ^{1}H-NMR (DMSO-d_6, 499.74 MHz): σ 8.56 (s, 4H), 7.20 (s, 8H), 5.21 (s, 4H), 3.90 (s, 2H). ^{13}C{^{1}H} NMR (DMSO-d_6,

125.67 MHz): σ 143.67, 141.50, 134.90, 129.57, 128.33, 47.74, 40.75. IR: Not collected as SCXRD provides clear visualization in a Chapter 3 crystal structure.

Synthesis of (ethyne-1,2-diylbis(4,1-phenylene))dimethanol (precursor to 3a): (ethyne-1,2-diylbis(4,1-phenylene))dimethanol (**3a precursor**) was prepared in bulk according to previously reported procedures.[14] 5.90 g (25.2 mmol) of (4-iodophenyl)methanol, 4.00 g (30.3 mmol) of (4-ethynylphenyl)methanol, 240 mg (1.26 mmol) of copper iodide, 884 mg (1.26 mmol) of bis(triphenylphosphine)palladium(II) chloride, 10.41 mL of triethylamine, and 150 mL of tetrahydrofuran were combined in a clean, dry 500 mL round bottom flask and stirred under nitrogen at room temperature for 48 hours. Upon completion as indicated *via* TLC, the resulting crude material was concentrated and dissolved in 300 mL of a 1:1 mixture of hexanes and ethyl acetate before running an 8 inch silica column in multiple 250 mL solutions of 20:1 hexanes/ethyl acetate. Fractions were confirmed pure *via* TLC, combined and dried under vacuum resulting in an off-white powder (6.16g, 85.0 % yield) 1H-NMR (DMSO-d_6, 499.74 MHz): σ 7.50 (d, J = 7.5 Hz , 4H), 7.36 (d, J = 7.4 Hz , 4H), 4.53 (s, 4H). $^{13}C\{^1H\}$ NMR (DMSO-d_6, 125.67 MHz): σ 143.82, 131.57, 127.08, 121.01, 89.50, 62.97. IR: 3317, 2885, 1515, 1410, 1212, 1180, 1100, 1044, 1027, 997, 952, 858, 840, 815, 774, 722, 642, 628, 614, 596, 579, 571, 560 cm^{-1}.

Synthesis of 1,2-bis(4-(bromomethyl)phenyl)ethyne (3a): 1,2-bis(4-(bromomethyl)phenyl)ethyne (**3a**) was prepared in bulk according to previously reported procedures.[15] 6.16 g (25.9mmol) of (ethyne-1,2-diylbis(4,1-phenylene))dimethanol, 15.0 mL (158 mmol) of phosphorus tribromide, and 100 mL of dichloromethane were combined in a clean, dry 250 mL round bottom flask, cooled in a methanol/ice bath and stirred under N_2 for 48 hours. Afterwards, the reaction was quenched with 150mL of ice water, separated with 200 mL

of dichloromethane, the organic phase was dried with magnesium sulfate, concentrated *in vacuo*, and the product was precipitated with 100 mL of diethyl ether as a bulky white powder. (5.01 g, 53.0% yield) ^{1}H-NMR ($CDCl_3$, 499.74 MHz): σ 7.43 (d, J = 7.4 Hz , 4H), 7.31 (d, J = 7.3 Hz , 4H), 4.42 (s, 4H). $^{13}C\{^{1}H\}$ NMR ($CDCl_3$, 125.67 MHz): σ 137.86, 131.90, 128.99, 123.13, 89.64, 32.82. IR: 3052, 2968, 2052, 1902, 1580, 1479, 1437, 1396, 1221, 1201, 1087, 1053, 1004, 956, 825, 796, 711, 665, 614, 588, 560 cm^{-1}.

Synthesis of 4,4'-((ethyne-1,2-diylbis(4,1-phenylene))bis(methylene))bis(1-(2-cyanoethyl)-4*H*-1,2,4-triazol-1-ium dibromide (3b): 5.00g (13.73 mmol) of 1,2-bis(4-(bromomethyl)phenyl)ethyne, 3.68g (30.21 mmol) of 3-(1H-1,2,4-triazol-1-yl)propanenitrile, and 150mL of acetonitrile were combined in a clean, dry 500 mL round bottom flask, and was refluxed for 18 hours. Upon completion, a white precipitate formed. The solids were removed via filtration, washed with 30 mL of acetonitrile 3 times, and dried under vacuum to yield a white fluffy powder. (1.98 g, 23% yield) ^{1}H-NMR (DMSO-d_6, 499.74 MHz): σ 10.24 (s, 2H), 9.41 (s, 2H), 7.65 (d, J = 7.6 Hz , 4H), 7.55 (m, J = 7.5 Hz , 4H), 5.61 (s, 4H), 4.72 (t, J = 4.7 Hz ,4H), 3.22 (t, J = 3.3 Hz , 4H). $^{13}C\{^{1}H\}$ NMR (DMSO-d_6, 125.67 MHz): σ 145.06, 143.45, 131.97, 131.70, 129.70, 129.14, 117.68, 47.23, 33.76, 17.30. IR: 3052, 2968, 2584, 1902, 1653, 1580, 1480, 1433, 1397, 1275, 1221, 1201, 1175, 1087, 1053, 1004, 956, 943, 872, 825, 796, 711, 668, 615, 588, 560 cm^{-1}.

Synthesis of 1,2-bis(4-((4*H*-1,2,4-triazol-4-yl)methyl)phenyl)ethyne (3c): To a clean, dry, 250 mL round bottom flask, 1.50 g (2.46 mmol) of 4,4'-((ethyne-1,2-diylbis(4,1-phenylene))bis(methylene))bis(1-(2-cyanoethyl)-4*H*-1,2,4-triazol-1-ium dibromide was suspended in 50 mL of a 6M solution of potassium hydroxide in water at reflux in a clean, dry, 250 mL round bottom flask overnight. Once the reaction reached completion, two separate

extractions took place. 100 mL of dichloromethane was added to the 50 mL potassium hydroxide solution and transferred to a separatory funnel for the first extraction. After three rinses with an additional 15 mL of dichloromethane, this organic layer was separated and concentrated under reduced pressure resulting in a crude oil. To the aqueous layer, 100 mL of ethyl acetate was added. The aqueous layer was then rinsed twice with an additional 2x25 mL of ethyl acetate. The organic ethyl acetate layer was then separated and dried under reduced pressure resulting in a crude oil. The two separate fractions of crude oil were then both redissolved in 50 mL of ethyl acetate, mixed, and dried over magnesium sulfate. This final organic layer was then concentrated, and a final purified product was precipitated out as a white powder using 50 mL of diethyl ether. (1.04 g, 81.0% yield) ^{1}H-NMR (DMSO-d_6, 499.74 MHz): σ 8.62 (s, 4H), 7.55 (d, J = 7.6 Hz , 4H), 7.32 (d, J = 7.3 Hz , 4H), 5.32 (s, 4H). ^{13}C{^{1}H} NMR (DMSO-d_6, 125.67 MHz): σ 143.36, 137.36, 131.85, 128.03, 121.82, 89.28, 47.23. IR: 3103, 1902, 1664, 1580, 1527, 1503, 1479, 1448, 1396, 1352, 1336, 1270, 1220, 1201, 1175, 1088, 1053, 1015, 1004, 978, 956, 852, 842, 824, 785, 750, 640, 629, 615, 588, 560 cm^{-1}.

Synthesis of 2,7-bis(bromomethyl)-9,10-dihydrophenanthrene (precursor to 4a): 2,7-bis(bromomethyl)-9,10-dihydrophenanthrene (**precursor 4a)** was prepared in bulk according to previously reported procedures.[16] 10.06 g (55.81 mmol) of 9,10-dihydrophenathrene, 7.36 g (245.4 mmol) of paraformaldehyde, 19.26 mL (354.6 mmol), 22.0 mL (386.2 mmol) of 33% HBr in glacial acetic acid and 11.0 mL (211.0 mmol) of 85% phosphoric acid were combined in a clean, dry, 500 mL round bottom flask and stirred under nitrogen at 80°C. After 21 hours, the reaction was brought to reflux for 5 hours, resulting in a grey solid. The supernatant liquid was decanted off and the grey solid was stirred in 150 mL of acetone at room temperature for 18 hours. The flask was then cooled to 0 °C and the reaction mixture was rinsed with 50 mL of -20

°C acetone, dried, and recrystallized using a mixture of 100 mL of 50/50 diethyl ether and petroleum ether. (3.88 g, 20% yield) ^{1}H-NMR (DMSO-d_6, 499.74 MHz): σ 7.82 (d, J = 7.8 Hz , 2H), 7.38 (m, J = 7.4 Hz , 2H), 7.36 (m, J = 7.3 Hz , 2H), 4.72 (s, 4H), 2.82 (s, 4H). ^{13}C{^{1}H} NMR (DMSO-d_6, 125.67 MHz): σ 137.87, 137.83, 133.90, 129.57, 128.56, 124.62, 35.02, 28.50. IR: 3031, 2924, 2893, 2830, 1893, 1585, 1485, 1428, 1416, 1303, 1240, 1160, 1099, 1031, 1006, 948, 913, 899, 871, 819, 744, 704, 661, 580, 555 cm^{-1}.

Synthesis of 2,7-bis(bromomethyl)phenanthrene (4a): 2,7-bis(bromomethyl)phenanthrene (**4a)** was prepared in bulk according to previously reported procedures.[17] 3.00g (8.24 mmol) of 2,7-bis(bromomethyl)-9,10-dihydrophenanthrene and 1.68g (7.41 mmol) of 2,3-dichloro-5,6-dicyano-1,4-benzoquinone were combined in a clean, dry, 500mL round bottom flask containing 100mL of dry benzene and brought to reflux for 18 hours. The crude mixture was filtered at 65 °C through a 2.5 inch column of neutral alumina with a vivid color change along the height of the column. The alumina was rinsed three times with 15 mL of 65°C hot benzene, the solvent was evaporated under reduced pressure, and the residue was recrystallized with 50 mL of petroleum ether to yield the product as white, airy crystals (1.66 g, 55.0% yield) To note, some peaks from (precursor **4a**) starting material are still present (reference ***Figure 15)***. ^{1}H-NMR (DMSO-d_6, 499.74 MHz): σ 8.82 (d, J = 8.9 Hz 2H), 8.07 (s, 2H), 7.87 (s, 2H), 7.75 (m, J = 7.8 Hz , 3H), 4.93 (s, 4H). ^{13}C{^{1}H} NMR (DMSO-d_6, 125.67 MHz): σ 137.22, 132.19, 129.30, 128.59, 127.66, 124.27, 38.88. IR: 3030, 2923, 2161, 1979, 1894, 1783, 1601, 1486, 1438, 1407, 1356, 1304, 1256, 1205, 1171, 1111, 1101, 947, 894, 874, 832, 806, 793, 743, 715, 692, 661, 617, 582, 553 cm^{-1}.

Synthesis of 4,4'-(phenanthrene-2,7-diylbis(methylene))bis(1-(2-cyanoethyl)-4*H*-1,2,4-triazol-1-ium) dibromide (4b): 1.25 g (3.43 mmol) of 2,7-bis(bromomethyl)phenanthrene, 922 mg (7.55 mmol) of 3-(1H-1,2,4-triazol-1-yl)propanenitrile, and 100 mL of acetonitrile were combined in a clean, dry 250 mL round bottom flask and refluxed for 18 hours. Upon completion, a white precipitate formed. The solids were removed via filtration, washed with 30 mL of acetonitrile 3 times, and dried under vacuum to yield a white fluffy powder. (crude yield: 1.63 g, 77.0%) There is some contamination from **4a** as the starting material is still present (reference ***Figure 15***) as well as undesired salt byproducts, all of which are extremely challenging to remove. ^{1}H-NMR (DMSO-d_6, 499.74 MHz): σ 10.36 (s, 2H), 9.50 (s, 2H), 8.97 (d, 2H), 8.11 (s, 1H), 7.91 (m, J = 7.9 Hz , 4H), 5.81 (s, 4H), 4.74 (t, J = 4.7 Hz , 4H), 3.24 (t, J = 3.2 Hz , 4H). ^{13}C{^{1}H} NMR (DMSO-d_6, 125.67 MHz): σ 145.18, 143.53, 137.73, 133.85, 132.94, 132.31, 131.81, 128.72, 127.19, 124.59, 124.31,117.70, 50.53, 47.26, 17.36. IR: 3018, 2974, 2256, 1568, 1520, 1487, 1438, 1407, 1366, 1340, 1308, 1229, 1175, 1145, 1066, 1011, 981, 920, 904, 822, 806, 748, 712, 697, 673, 624, 565 cm^{-1}.

Synthesis of 2,7-bis((4*H*-1,2,4-triazol-4-yl)methyl)phenanthrene (4c): To a clean, dry, 100mL round bottom flask, 1.00g (1.64 mmol) of 4,4'-(phenanthrene-2,7-diylbis(methylene))bis(1-(2-cyanoethyl)-4*H*-1,2,4-triazol-1-ium) dibromide was suspended in 50 mL of a 6M solution of potassium hydroxide in water at reflux in a clean, dry, 250 mL round bottom flask overnight. Once the reaction reached completion, two separate extractions took place. 50 mL of dichloromethane was added to the 50 mL potassium hydroxide solution and transferred to a separatory funnel for the first extraction. After three rinses with an additional 15 mL of dichloromethane, this organic layer was separated and concentrated under reduced pressure resulting in a crude oil. To the aqueous layer, 50 mL of ethyl acetate was added. The

aqueous layer was then rinsed twice with an additional 2x15 mL of ethyl acetate. The organic ethyl acetate layer was then separated and dried under reduced pressure resulting in a crude oil. The two separate fractions of crude oil were then both redissolved in 50 mL of ethyl acetate, mixed, and dried over magnesium sulfate. The final organic layer was then dried over magnesium sulfate, concentrated and then precipitated out as a white powder using diethyl ether, ethanol, and isopropyl alcohol. (50 mg, <5% yield) To note, this organic linker is extremely hygroscopic and as such rinsing with various different "wet" solvents rinses away a bulk amount of product. This organic linker also has issues with solubility as it is miscible in many solvents which led to both extraction and purification issues. As a second note, some peaks from (precursor **4a**) starting material are still present (reference ***Figure 15)*** in this product, however, many of the undesired salt byproducts have been removed. ^{1}H-NMR (DMSO-d_6, 499.74 MHz): σ 8.83 (d, J = 8.8 Hz , 2H), 8.7 (s, 4H), 7.80 (s, 4H), 7.62 (d, J = 7.6 Hz , 2H), 7.22 (d, J = 7.2 Hz , 2H), 5.50 (s, 4H). ^{13}C{^{1}H} NMR (DMSO-d_6, 125.67 MHz): σ 143.87, 135.83, 133.63, 129.57, 127.74, 126.90, 124.37, 47.96. IR: 3387, 3018, 2974, 2256, 1622, 1568, 1526, 1486, 1438, 1407, 1366, 1339, 1308, 1252, 1229, 1177, 1145, 1074, 979, 920, 903, 822, 806, 748, 696, 673, 624, 570, 564, 550 cm^{-1}.

References

1. Jia, J.-G. and Zheng, L.-M. “Metal-Organic Nanotubes: Designs, Structures and Functions” *Coordination Chemistry Reviews* 403, **2020**: 213083.

2. Otsubo, K.; Wakabayashi, Y.; Ohara, J.; Yamamoto, S.; Matsuzaki, H.; Okamoto, H.; Nitta, K.; Uruga, T.; Kitagawa, H. Bottom-up realization of a porous metal–organic nanotubular assembly. *Nature Materials* **2011**, *10*, 291–295.

3. Vailonis, K. M., Gnanasekaran, K., Powers, X. B., Gianneschi, N. C., and Jenkins, D. M. “Elucidating the Growth of Metal–Organic Nanotubes Combining Isoreticular Synthesis with Liquid-Cell Transmission Electron Microscopy” *Journal of the American Chemical Society* 141, no. 26 (**2019**): 10177–10182.

4. Furukawa, H.; Cordova, K. E.; O’Keeffe, M.; Yaghi, O. M. The Chemistry and Applications of Metal-Organic Frameworks. *Science* **2013**, *341* (6149).

5. Thanasekaran, P.; Luo, T.-T.; Lee, C.-H.; Lu, K.-L. A journey in search of single-walled metal-organic nanotubes. *Journal of Materials Chemistry* **2011**, *21* (35), 13140–13149.6.

6. Panda, T.; Kundu, T.; Banerjee, R. Self-assembled one dimensional functionalized metal–organic nanotubes (MONTs) for proton conduction. *Chemical Communications* **2012**, *48* (44), 5464–5466.

7. Murdock, C. R.; Jenkins, D. M. Isostructural Synthesis of Porous Metal–Organic Nanotubes. *Journal of the American Chemical Society* **2014**, *136* (31), 10983–10988.

8. Adarsh, N. N.; Dîrtu, M. M.; Naik, A. D.; Léonard, A. F.; Campagnol, N.; Robeyns, K.; Snauwaert, J.; Fransaer, J.; Su, B. L.; Garcia, Y. Single-Walled Metal–Organic Nanotube Built from a Simple Synthon. *Chemistry – A European Journal* **2015**, *21* (11), 4300–4307

9. Li, H.; Eddaoudi, M.; O'Keeffe, M.; Yaghi, O. M.,Design and synthesis of an exceptionally stable and highly porous metal-organic framework. Nature 1999, 402, 276-279;

10. Eddaoudi, M.; Kim, J.; Rosi, N.;Vodak, D.; Wachter, J.; O'Keeffe, M.; Yaghi, O. M., Systematic Design of Pore Sizeand Functionality in Isoreticular MOFs and Their Application in Methane Storage. Science 2002, 295, 469-472.

11. Tagat, J. R.; McCombie, S. W.; Barton, B. E.; Jackson, J.; Shortall, J. Synthetic Inhibitors of Interleukin-6 II: 3,5-Diaryl Pyridines and Meta-Terphenyls. *Bioorganic & Medicinal Chemistry Letters* **1995**, *5* (18), 2143–2146

12. Banfi, S.; Montanari, F.; Pozzi, G.; Quici, S. Dimeric Mn(Iii)-Tetraarylporphyrins as Catalysts for H2O2-Promoted Olefin Epoxidation. *Tetrahedron* **1994**, *50* (30), 9025–9036.

13. Peng, K.-Y.; Chen, S.-A.; Fann, W.-S. Efficient Light Harvesting by Sequential Energy Transfer across Aggregates in Polymers of Finite Conjugational Segments with Short Aliphatic Linkages. *Journal of the American Chemical Society* **2001**, *123* (46), 11388–11397.

14. Hayashi, H.; Yamada, T.; Kitoh, A.; Mizutani, Y.; Futamura, M.; Onouchi, Y.; Hirano, K.; Miyake, T. Synthesis of Acetylene-Containing Polyurethanes and Their Strain Sensing Property with Micro-Raman Spectroscopy. *Journal of The Adhesion Society of Japan* **2012**, *48* (3), 103–108.

15. Adam, A.; Haberhauer, G. Twisting of Alkynes towards a Carbon Double Helix. *Chemistry – A European Journal* **2017**, *23* (50), 12190–12197.

16. Loots, L.; Barbour, L. J. An Infinite Catenane Self-Assembled by Π···π Interactions. *Chem. Commun.* **2013**, *49* (7), 671–673.

17. Muppidi, A.; Doi, K.; Ramil, C. P.; Wang, H.-G.; Lin, Q. Synthesis of Cell-Permeable Stapled BH3 Peptide-Based MCL-1 Inhibitors Containing Simple Aryl and Vinyl aryl Cross-Linkers. *Tetrahedron* **2014**, *70* (42), 7740–7745.

18. Jin, J.-C.; Wang, Y.-Y.; Liu, P.; Liu, R.-T.; Ren, C.; Shi, Q.-Z. An Unusual Independent 1D Metal−Organic Nanotube with Mesohelical Structure and 1D → 2D Interdigitation. *Crystal Growth & Design* **2010**, *10* (5), 2029–2032.

19. Jayasinghe, A. S.; Unruh, D. K.; Kral, A.; Libo, A.; Forbes, T. Z. Structural Features in Metal–Organic Nanotube Crystals That Influence Stability and Solvent Uptake. *Crystal Growth & Design* **2015**, *15* (8), 4062–4070.

20. Green, M. L. and Parkin, G. Application of the Covalent Bond Classification Method for the Teaching of Inorganic Chemistry *Journal of Chemical Education* 91, no. 6 (**2014**): 807–816.

21. Hu, G., Liu, Q., Zhou, Y., Yan, W., Sun, Y., Peng, S., Zhao, C., Zhou, X., and Deng, H. Extremely Large 3D Cages in Metal–Organic Frameworks for Nucleic Acid Extraction *Journal of the American Chemical Society* 145, no. 24 (**2023**): 13181–13194.

22. Jia, J.-G. and Zheng, L.-M. Metal-Organic Nanotubes: Designs, Structures and Functions *Coordination Chemistry Reviews* 403, (2020): 213083.

CHAPTER 3

SYNTHESIS OF METAL-ORGANIC NANOTUBES WITH EXPANDED PORE

Abstract

Metal organic nanotubes (MONTs) are a 1-dimensional subcategory derived from metal organic frameworks. Despite being in a juvenile stage, MONTs have currently sparked an interest in the field of porous materials as a class of materials that encompasses characteristics of both MOFs and CNs. In order to further develop this class of materials, increasing the size of these materials is imperative as it will increase their overall uses and routes of adaptation. The studies discussed in this chapter are preliminary investigations towards MONTs as a large-pored material and the revelations that can be made from these discoveries.

Introduction

Metal organic nanotubes (MONTs) consist of three segments, an organic segment which acts as the backbone of the pore (refer to **Figure 6a**), a metal center (refer to **Figure 6b**) which acts as an anchor further providing structure to the synthesized nanotube, and an anionic cap (refer to **Figure 6b**) which acts as a closing agent for the nanotube. The function of any material is based on its dimensionality and with this being said, work highlighted in chapter 2 is only one half of the necessary puzzle for synthesis of expanded pore MONTs. When reflecting on previous work accomplished by Chris Murdock and Kristina Vailonis, pathways for MONT synthesis with multi-phenyl organic systems were investigated and optimized.[1-4] When reflecting on MONTs as a subclass of metal organic frameworks (MOFs) important considerations were made. To highlight, when a pore size is deliberately tuned a direct effect on the properties of the synthesized material also occurs.

Chris Murdock's MONTs were expandable porous material, primarily synthesized utilizing two different organic linkers, one of which was a mono-phenyl organic system, and the other was a naphthyl organic system.[1,4] Utilizing key characteristics of the synthesized silver-

based MONTs, Murdock was able to pave the way for how this subcategory of MOF could be classified. Using a combination of powder x-ray diffraction (PXRD), single crystal x-ray diffraction (SCXRD), thermogravimetric analysis (TGA) and gas adsorption complete characterization was obtained. Shown in ***Figure 16***, as an organic linker increases in size, the amount of adsorbed gas a pore can withhold also reflects this increase.[1,4]

As a porous material increases in size, there are certain ideal applications that make the synthesis and discovery of these materials worth investigating. These applications may include but are not limited to, gas storage, gas separations, heterogeneous catalysis, homogeneous catalysis, and external site modification post-synthesis. Herein this chapter, a focus on the synthesis of expanded moiety MONTs is investigated and key conclusions drawn using PXRD, SXRD, TGA and gas adsorption are discussed.

Results and Discussion

Metal organic nanotubes (MONTs) have been prepared and synthesized utilizing many different organic linkers, metal centers, and capping agents. It is, however, important to distinguish the different methods of synthesis and how each one leads to a different molecular structure. Multiple groups each spearheaded by their own respective principal investigator, observed three main ways in which MONTs can be classified. These specific classes of MONTs are broken into the two-column, three-column, and four-column pillared approaches. In the past, the utilization of di-triazole organic linkers aided in gave birth to the 2-column pillared approach which is known for its capabilities for height and width independent adjustment. Following in the footsteps of past group members semi-ridgid di-triazole organic linkers were utilized to develop MONTs with an expanded pore size. It is significant to note however, that the organic

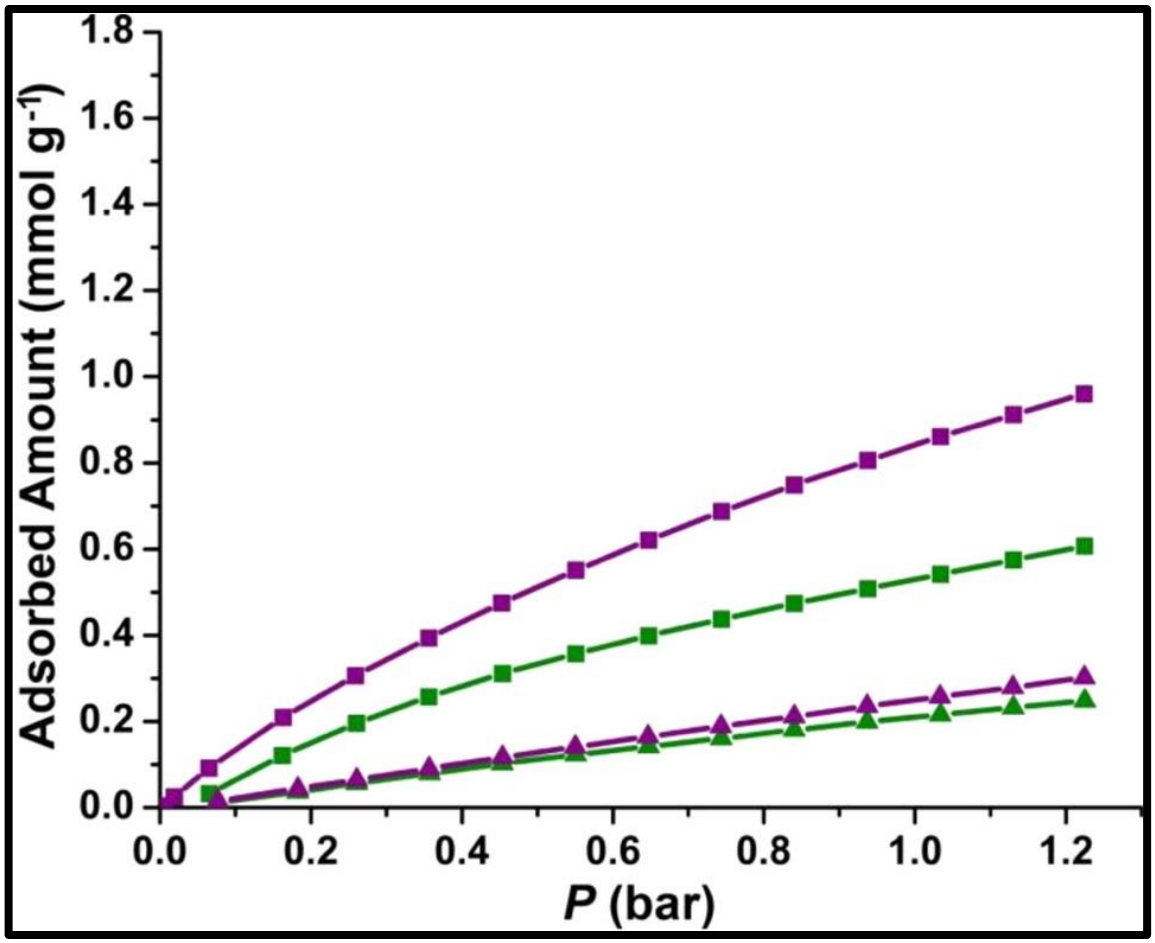

Figure 16. **CO_2 (squares) and CH_4 (triangles) adsorption isotherms for phenyl and naphthyl based-MONTs where phenyl (green) and naphthyl (purple) show as a pore increases the level of adsorbed gas also increases.**

linkers selected would result in data that reflects one of the largest pores ever synthesized when looking at the two-column pillared approach. Two-column pillared MONTs synthesized by group members of the past utilized a 1,3-bis((4*H*-1,2,4-triazol-4-yl)methyl)benzene organic linker, and a group 11 metal salt which formed one of the first MONTs of its kind.[1-4] Two of the metal salts that had the greatest success were $CuBr_2$ and $AgNO_3$ which provided the skeletal structure for the future of MONTs synthesized within the Jenkins group.[4] Referring back to these previously accomplished syntheses, it was important to generate results using a smaller organic linker before delving into the synthesis of a MONT with an expanded organic linker.

Shown in ***Figure 17***, MONT $Cu_2(L0_a)Cl_2$ was synthesized using organic linker 1,3-bis((4*H*-1,2,4-triazol-4-yl)methyl)benzene and a $CuCl_2$ metal salt. The resulting MONT was synthesized in a 1:1 volumetric ratio with concentrations ranging between that of a 10mM organic linker to 20-50mM of metal salt. With multiple duplicate results, a large, thin crystal was selected for SCXRD analysis which upon completion a pore width of 9.306Å and a pore height of 10.468Å was determined. When drawing comparisons between the 1,3-bis((4*H*-1,2,4-triazol-4-yl)methyl)benzene MONT synthesized by Chris Murdock and the 1,3-bis((4*H*-1,2,4-triazol-4-yl)methyl)benzene MONT I synthesized, an extremely minor 0.02Å width difference was visualized.[4] Using the two-column pillared approached it was primarily thought that MONTs synthesized relied on the selection of organic linker and the metal center, but these preliminary results might suggest that the anionic cap also has some influence on how large or how small a pore might be.[4-8] Moving forward, a repertoire was established that MONTs could be synthesized under a variety of different conditions that were not originally specified, however one key component remained which stated the metal salt would almost always need to be used in excess in order to develop a MONT structure.[4-8] Prioritizing the lessons learned on small organic linker

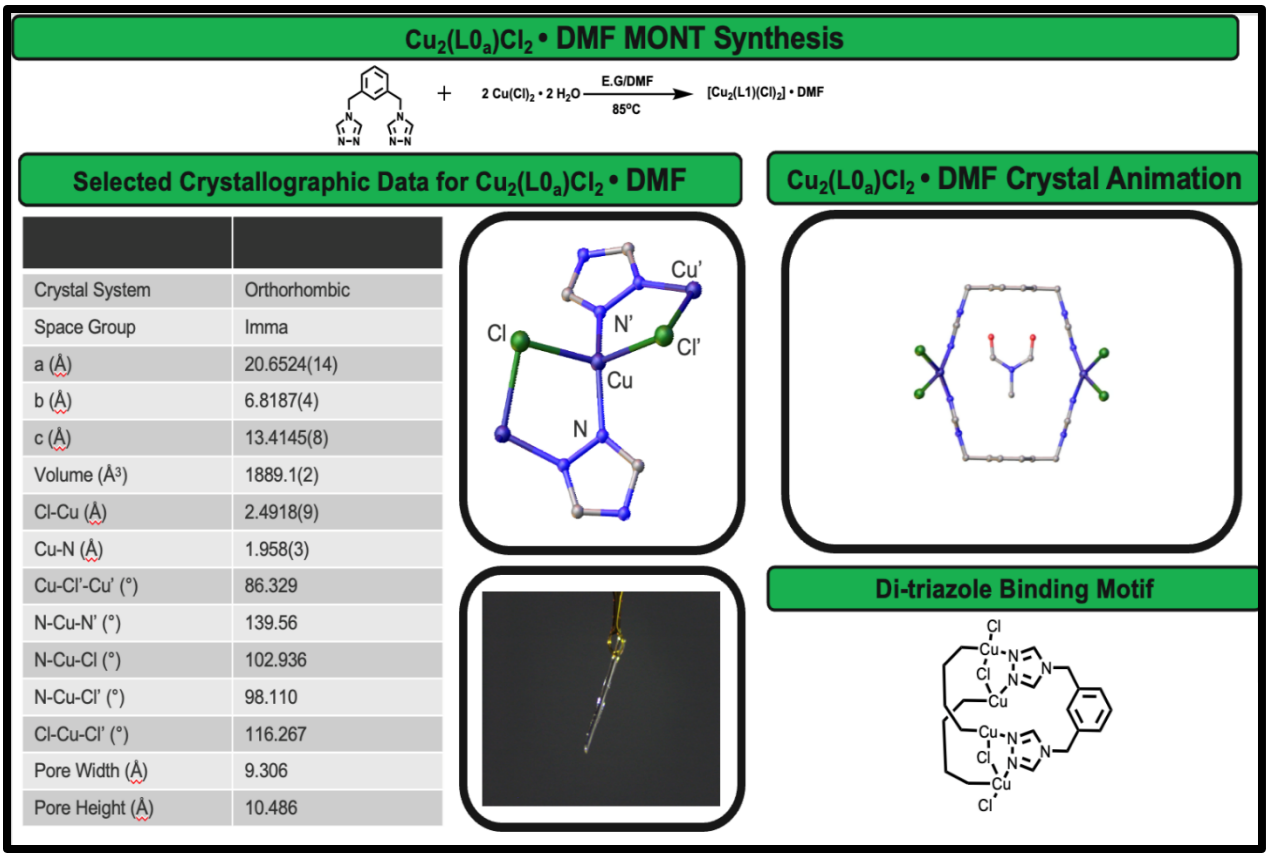

Figure 17. **Utilizing organic linker 1,3-bis((4*H*-1,2,4-triazol-4-yl)methyl)benzene which was first developed by Dr. Chris Murdock, a new two-column pillared MONT was synthesized using $CuCl_2$ as the metal salt. Carbon (grey), Nitrogen (blue), Copper (Purple), Chloride (green), and Oxygen (red) are shown on SCXRD animations.**

MONT synthesis, applying this knowledge to the synthesis of an expanded pore MONT was possible and from this knowledge a boon of many thousands of reactions occurred resulting in results that ranged from inconclusive to conclusive.

Shown in ***Figure 18***, MONT $Cu_2(L1_d)Cl_2$ was synthesized using organic linker 4,4"-bis((4*H*-1,2,4-triazol-4-yl)methyl)-1,1':3',1"-terphenyl and a $CuCl_2$ metal salt. The resulting MONT was synthesized in a 1:1 volumetric ratio with concentrations ranging between that of 2-10mM of organic linker to 20-50mM of metal salt. This particular MONT yielded crystals that were short, thin and had a gentle green hue. This particular crystal had extensive synthetic challenges to overcome with a time lapse of approximately one year. Using a small 4 mL dram, 1mL of 4,4"-bis((4*H*-1,2,4-triazol-4-yl)methyl)-1,1':3',1"-terphenyl dissolved in dimethylformamide and 3mL of $CuCl_2$ dissolved in water were mixed and heated for one week at 85 °C. Generated from reaction conditions that were thought to be invaluable, the first preliminary structure generated for this crystal occurred in October of 2023 which had an R_1 value of 12.27 with multiple A-level errors making it effectively unpublishable. From this point forward replication of this crystal was an absolute must, and as such utilizing the same reaction conditions as set prior had occurred. For this first preliminary structure, a volumetric ratio of 1:3 with concentrations of 10 mM of organic linker to 90 mM of metal salt were employed and reran in multiple batches to form duplicate results. However, after hundreds of tests using the same conditions no repeatable results were accomplished. Thinking back to lessons learned on the MONT synthesized using a small organic linker, changing the reaction conditions was the only foreseeable way forward, and from this, exceptional results occurred. Shown in ***Table 1,*** a myriad of reaction conditions were testing resulting in hundreds of samples produced. Using the organic linker 4,4"-bis((4*H*-1,2,4-triazol-4-yl)methyl)-1,1':3',1"-terphenyl in combination with

Table 1. **Organic linker 4,4''-bis((4*H*-1,2,4-triazol-4-yl)methyl)-1,1':3',1''-terphenyl used in conjunction with many group 11 metal salts. Results highlighted in red indicate conditions where crystals were grown and the numerical values indicated in this table are how many vials were set over the course of a year long period. Over 1000 vials were tested and of that, approximately 18% of vials used had grown a crystalline material that was reasonable for analysis.**

Concentrations of Ligand to Metal	$CuBr_2$	$CuCl_2$	$CuNO_3$	$AgNO_3$
2mM to 20mM	24	24	6	6
2mM to 40mM	24	24	6	6
2mM to 80mM	24	24	6	6
5mM to 20mM	96	96	6	6
5mM to 40mM	96	96	6	6
5mM to 80mM	24	24	6	6
10mM to 20mM	120	120	6	6
10mM to 40mM	120	120	6	6
10mM to 80mM	24	24	6	6

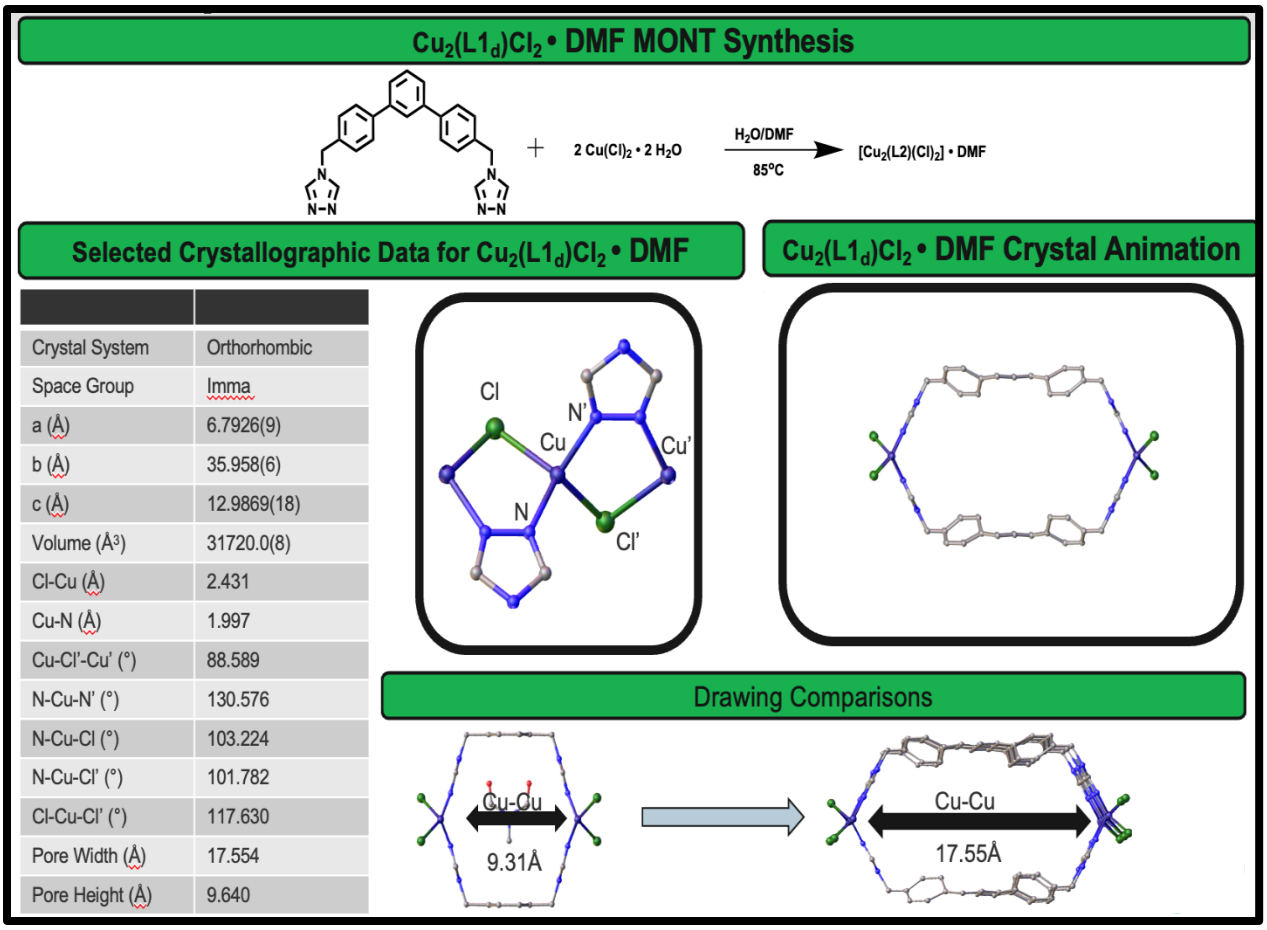

Crystal System	Orthorhombic
Space Group	Imma
a (Å)	6.7926(9)
b (Å)	35.958(6)
c (Å)	12.9869(18)
Volume (Å^3)	31720.0(8)
Cl-Cu (Å)	2.431
Cu-N (Å)	1.997
Cu-Cl'-Cu' (°)	88.589
N-Cu-N' (°)	130.576
N-Cu-Cl (°)	103.224
N-Cu-Cl' (°)	101.782
Cl-Cu-Cl' (°)	117.630
Pore Width (Å)	17.554
Pore Height (Å)	9.640

Figure 18. **Utilizing organic linker 4,4''-bis((4*H*-1,2,4-triazol-4-yl)methyl)-1,1':3',1''-terphenyl and $CuCl_2$ as the metal salt, one of the largest two-column pillared MONTs was synthesized resulting in an approximate 50% size increase along its width. Carbon (grey), Nitrogen (blue), Copper (Purple), Chloride (green), and Oxygen (red) are shown on SCXRD animations.**

Reflected in ***Figure 18*** and ***Table 1***, replicating this MONT was exceptionally challenging but after many runs a crystal large enough for analysis was obtained approximately one year after the first preliminary $Cu_2(1_d)Cl_2$ MONT structure. Using a 1:1 volumetric ratio with a 1:4 concentration (L:M), a duplicate crystal was grown and analyzed using SCXRD which resulted in calculated R_1 value of 3.88 and no A-level errors. With publishable SCXRD data it was possible to move forward with other forms of characterization which included powder X-ray diffraction (PXRD), thermogravimetric analysis (TGA), infrared spectroscopy (IR), and gas adsorption. Represented in ***Figure 19***, powder X-ray diffraction was used in order to confirm that the experimental bulk phase matched with the simulated bulk phase which was calculated from SCXRD data. Once the bulk phase was confirmed a match with the SCXRD data, the next segment of experimentation took place.

In order to accomplish solvent exchange, approximately 100 mg of bulk $Cu_2(1_d)Cl_2$ was placed in a 20mL vial which was then covered with a layer of methanol and a cap was gently placed over the top of the vial. The top of the vial was not screwed down as for the solvent exchange to occur methanol needed to evaporate at a slow rate over multiple 8 hour segments. Setting a heating mantle to approximately 50 °C under these conditions allowed for the slow evaporation of the methanol layer and this was repeated three times over the course of 48 hours. A replicate PXRD was taken in order to confirm that the structural integrity of the bulk phase was not compromised and from these results conclusions were drawn that upon solvent exchange a sharpening of powder peaks could be observed.

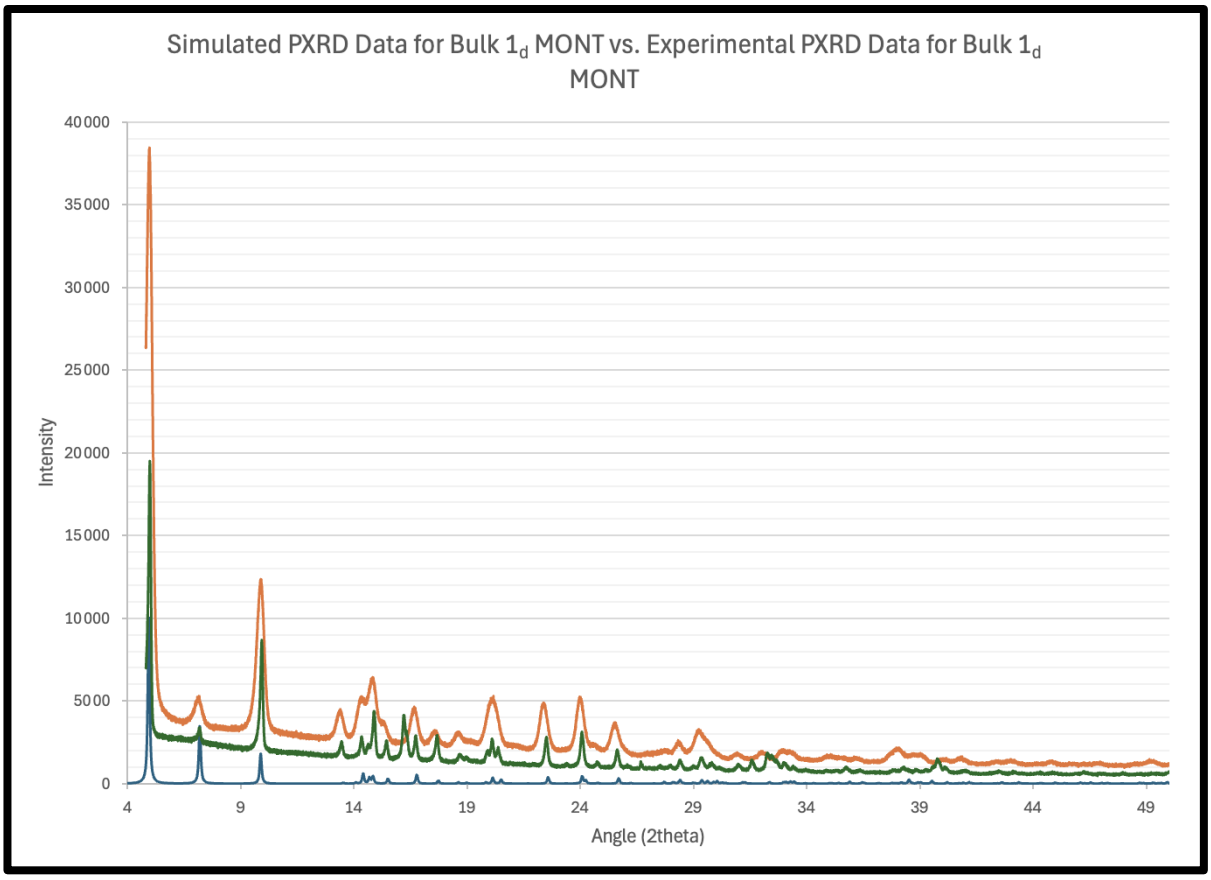

Figure 19. **Stacked PXRD data for $Cu_2(1_d)Cl_2$ MONT where simulated (blue), experimental (green), and solvent exchanged (orange) peaks are indicated.**

A key component of analysis for MONTs lies in determining at which temperature does the structural integrity of the MONT collapse. Utilizing thermogravimetric analysis, ***Figure 20a*** and ***20b*** show two different series in which the first post-solvent exchanged sample shows thermal stability upwards of 200 °C and the pre-solvent exchanged sample shows a thermal stability upwards of 150 °C. With these two conditions defined, it was possible to create a set of experimental conditions for running gas adsorption. With the bulk phase material, a ~120 mg sample was loaded into the gas adsorption where three different gases were utilized for testing each of which providing their own unique set of results. Shown in ***Figure 21***, little to no porosity can be observed when looking at each gas tested. A PXRD was taken on the sample post-analysis which had shown peak broadening. This broadening suggests a diminishment in porosity of the MONT. Some conclusions can be made where although pore size can be visualized on SCXRD, applying pressure to these expanded pore MONTs utilizing gas adsorption can lead to structural failure of the MONT.

As synthesis towards the expanded pore goal continued, one other organic linker provided promising results. Shown in ***Table 2***, organic linker bis(4-((4*H*-1,2,4-triazol-4-yl)methyl)phenyl)methane was mixed in a 1:3 volumetric ratio with a concentration of 10 mM organic linker to 90 mM of $CuCl_2$ metal salt. The following crystal that had grown in solution was clear, large and had a star-like appearance before fragmentation for SCXRD and PXRD analysis. With a pore width of 15.480 Å and a pore height of 7.250 Å this sheet-like (MOF) crystal structure (shown in ***Figure 22***) represents quality preliminary data which aids in the supporting the claim that the use of expanded organic linkers leads to crystalline material with pore widths exceeding 15.00 Å. Synthesized in a series of 6, 4 mL vial equivalent portions, a bulk solution of $Cu_2(2c)Cl_2$ was prepared for PXRD analysis.

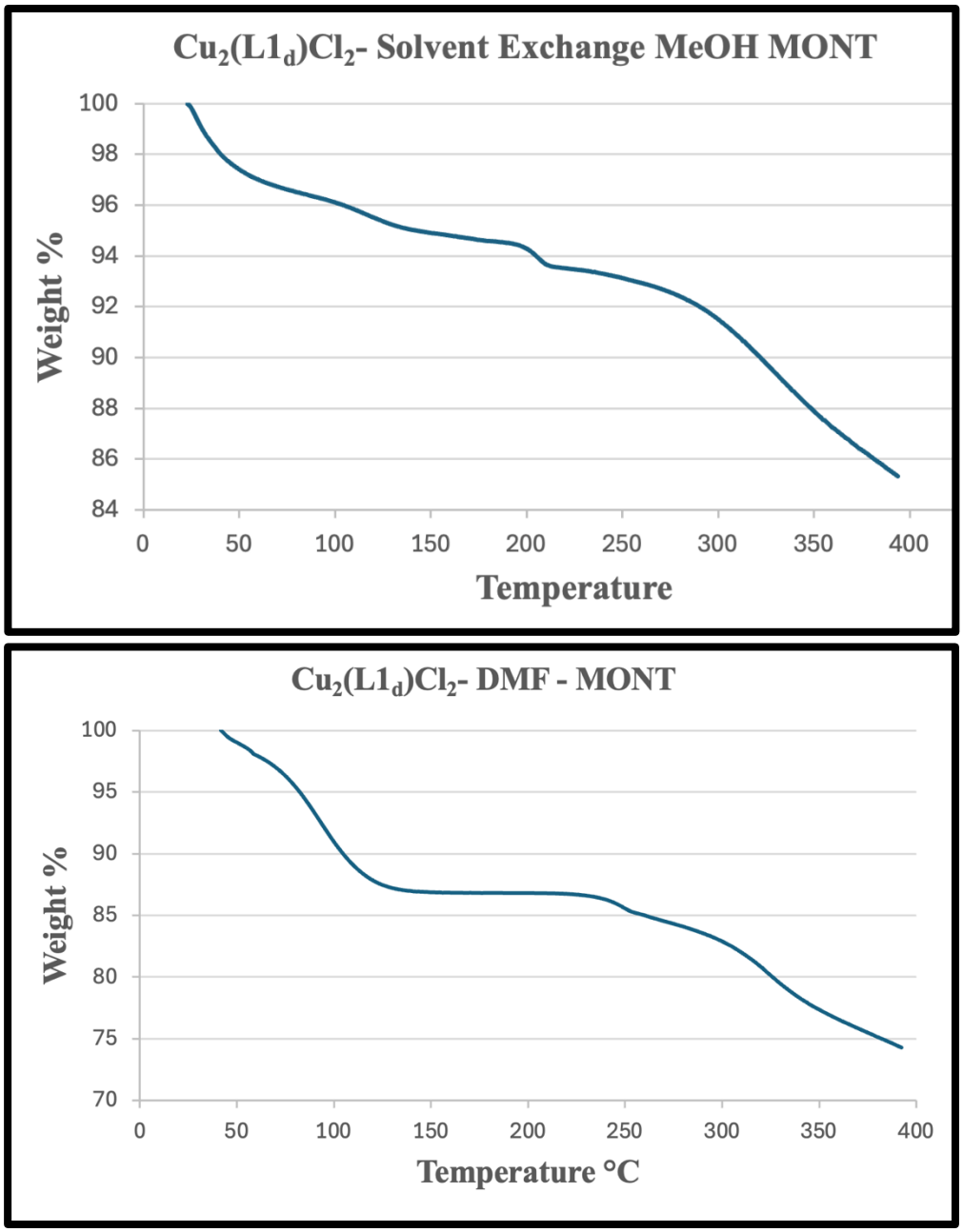

Figure 20 (a) and 20 (b). **TGA data for MONT $Cu_2(L1_d)Cl_2$ which shows thermal stability in both pre and post-solvent exchanged conditions.**

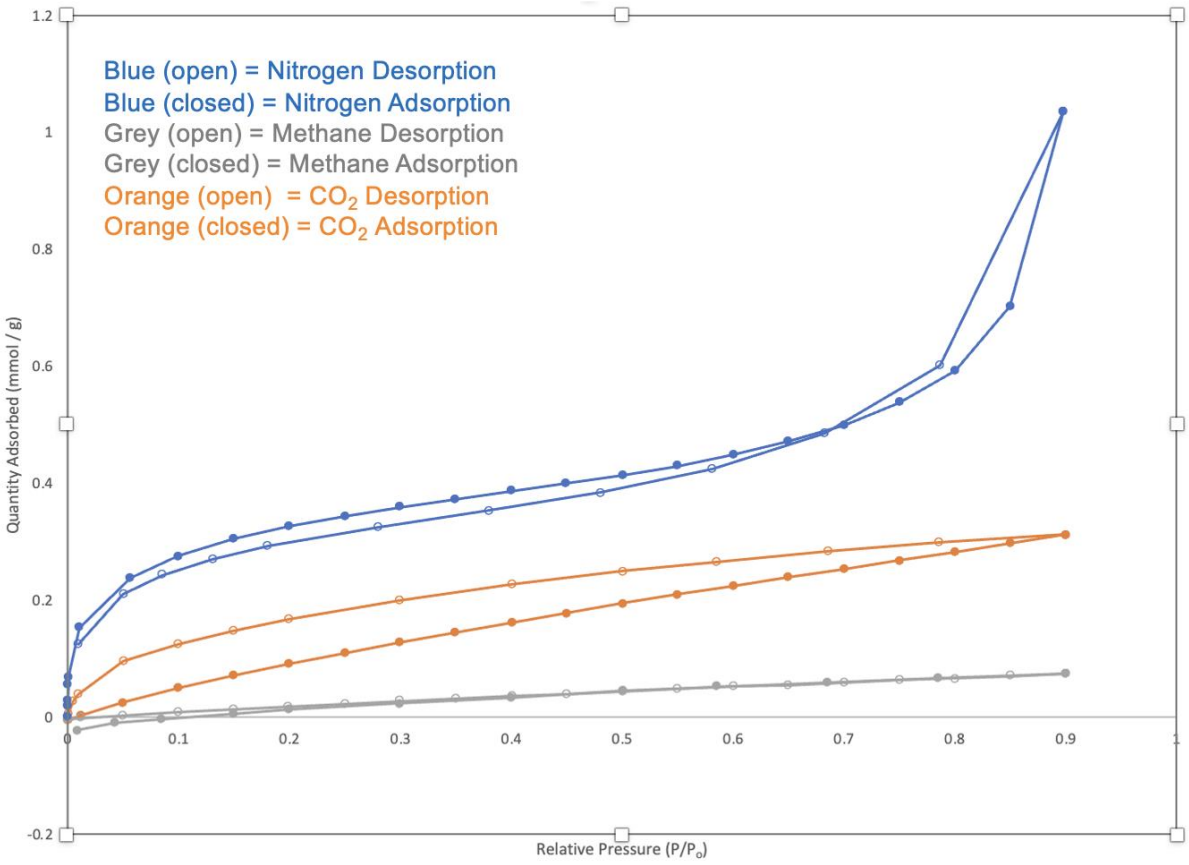

Figure 21. **Gas Adsorption data representing little to no porosity may suggest MONTs which when formed utilizing an expanded pore, have structural complications where when put under pressure may lead to collapse.**

Table 2. **Organic linker bis(4-((4*H*-1,2,4-triazol-4-yl)methyl)phenyl)methane used in conjunction with many group 11 metal salts. Results highlighted in red indicate conditions where crystals were grown and the numerical values indicated in this table are how many vials were set over the course of a year long period. Of the over 1200 vials that were tested, approximately 8% of vials used had grown a crystalline material that was reasonable for analysis.**

Concentrations of Ligand to Metal	$CuBr_2$	$CuCl_2$	$CuNO_3$	$AgNO_3$
5mM to 20mM	96	96	6	6
5mM to 40mM	96	96	6	6
5mM to 80mM	24	24	6	6
10mM to 20mM	120	120	6	6
10mM to 30mM	60	48	6	6
10mM to 40mM	120	120	6	6
10mM to 80mM	24	24	6	6
10mM to 90mM	48	60	6	6

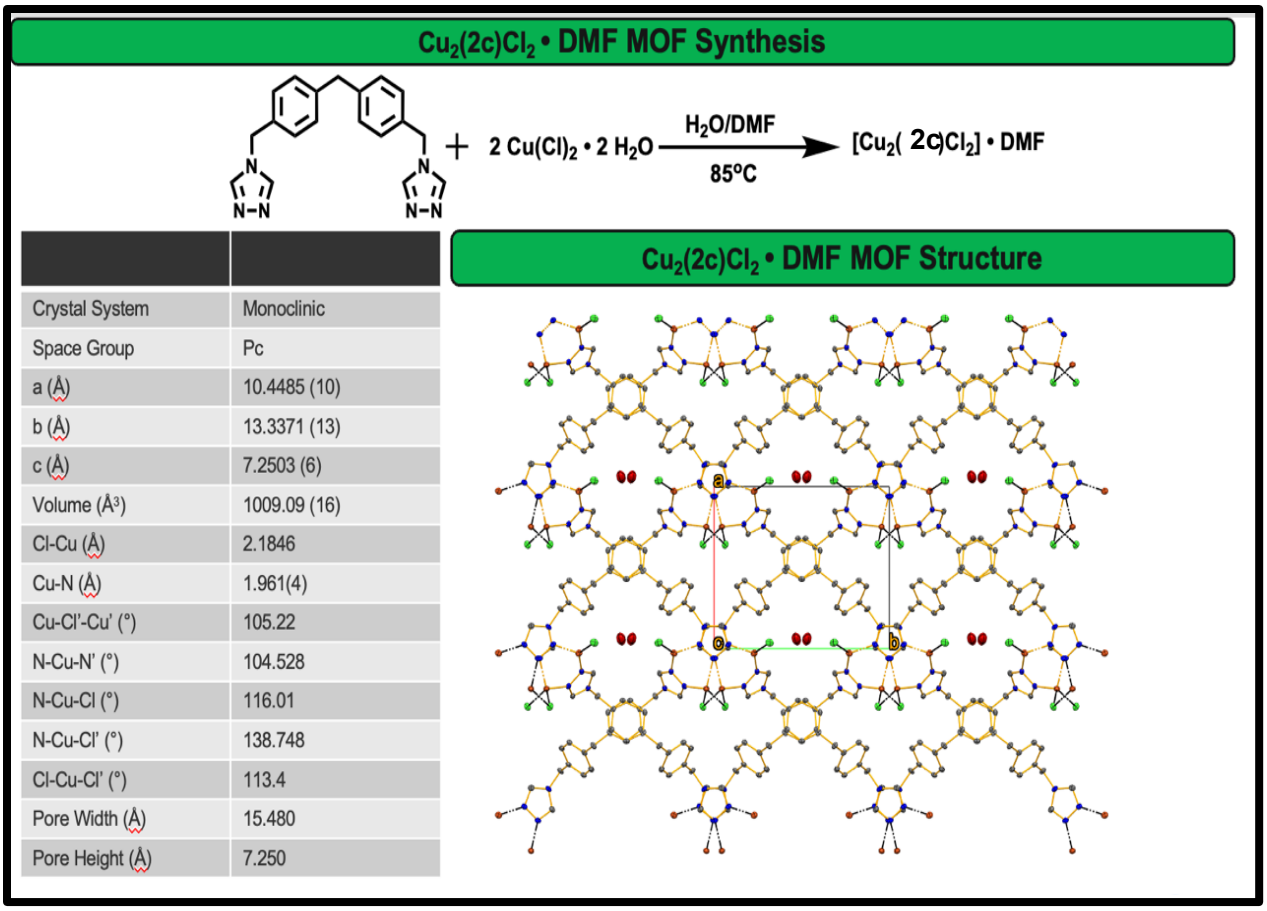

Figure 22. **Utilizing organic linker bis(4-((4*H*-1,2,4-triazol-4-yl)methyl)phenyl)methane and $CuCl_2$ as the metal salt, preliminary data reflecting a 2D interlocked MOF structure was obtained. Carbon (grey), Nitrogen (blue), Copper (Orange), Chloride (green), and Oxygen (red) are shown on SCXRD animations. Pore width similar to that of MONT $Cu_2(1_d)Cl_2$ is observed with a difference of ~2 Å, however, as this is a 2D structure it cannot be considered a true MONT.**

To a clean, heated 20 mL vial, 33.4mg of bis(4-((4*H*-1,2,4-triazol-4-yl)methyl)phenyl)methane was dissolved in 10 mL of dimethylformamide at 85 °C. To a second clean, heated 20 mL vial, 105 mg of $CuCl_2$ was dissolved in 20 mL of water at 85 °C. Mixing the two solutions at 85 °C for three days in a heating block with a volumetric ratio of 1:3 yielded large, clear crystals which were then rinsed with hot dimethylformamide, hot water, and a small amount of acetone. This collection of bulk phase crystal was then ground into a fine powder before analysis using PXRD. Drawing comparisons between the simulated PXRD data and the experimental PXRD data (shown in ***Figure 23***) closing remarks towards this MOF can be made.

Although this crystal structure did not form a 1D MONT, it still provided important insights towards the use of bis(4-((4*H*-1,2,4-triazol-4-yl)methyl)phenyl)methane as an organic linker for crystal synthesis. With this particular organic linker, a connecting methylene bridge was hypothesized to have too many degrees of free rotation, which was later supported based on the results of SCXRD analysis. Although this organic linker may not have been a complete success, it aiding in building a pathway towards selecting organic linkers that have stronger rigidity about the central moiety.

Applying learned concepts from MONT 1_d and MOF 2c, two other organic linkers were evaluated for crystal synthesis. Organic linkers 1,2-bis(4-((4*H*-1,2,4-triazol-4-yl)methyl)phenyl)ethyne and 2,7-bis((4*H*-1,2,4-triazol-4-yl)methyl)phenanthrene were both used in conjunction with many different metal salts (shown in ***Table 3 and 4)*** resulting in inconclusive data. Following a series of synthetic methods as proposed with MONT 1_d and MOF 2c, between the two organic linkers over 1000 vials were prepared, observed under a microscope, and charted. Many different colors were observed ranging from white, to green, to blue, to dark

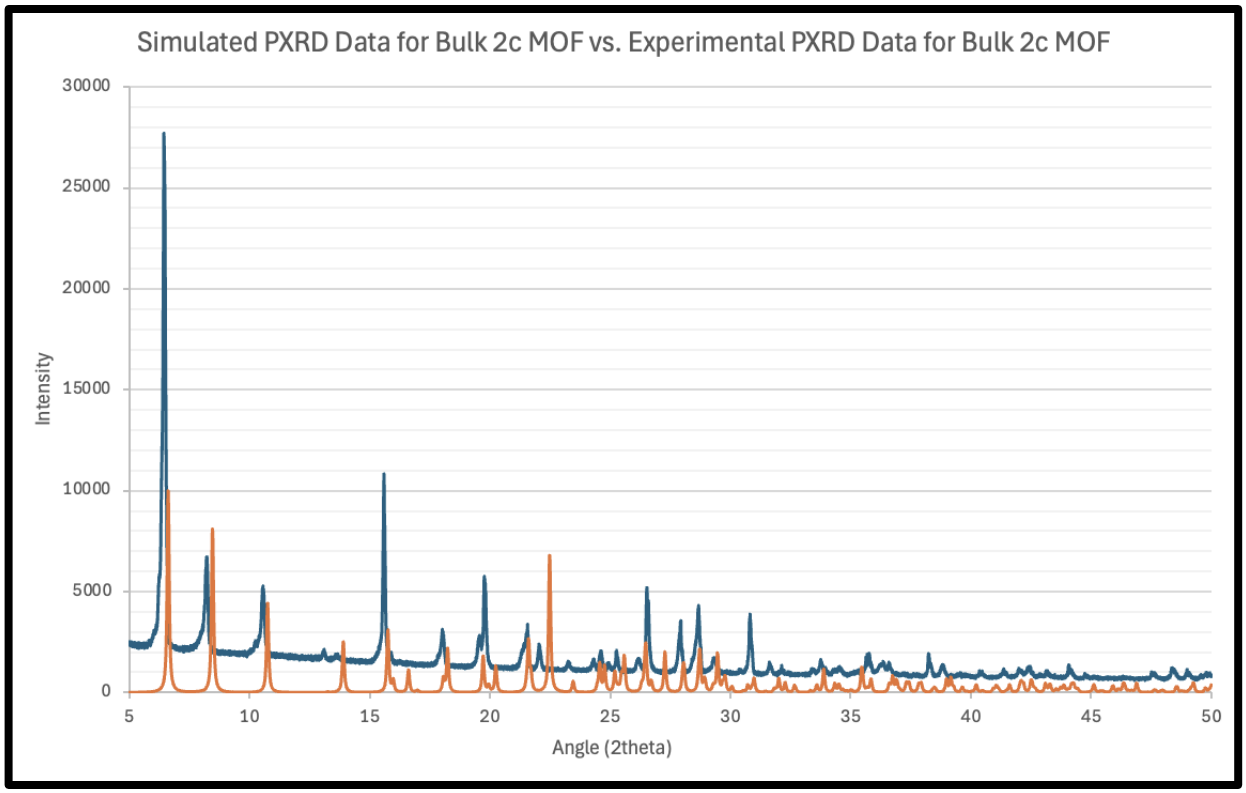

Figure 23. **Stacked PXRD data for $Cu_2(2c)Cl_2$ MOF where simulated (orange) and experimental (blue) peaks are indicated.**

Table 3. **Organic linker 1,2-bis(4-((4*H*-1,2,4-triazol-4-yl)methyl)phenyl)ethyne used in conjunction with many group 11 metal salts. Results highlighted in red indicate conditions where crystals were grown and the numerical values indicated in this table are how many vials were set over the course of a year long period. Of the over 500 vials that were tested, there was no crystalline material that was synthesized on a large enough scale that could be used for SCXRD analysis.**

Concentrations of Ligand to Metal	**$CuBr_2$**	**$CuCl_2$**	**$CuNO_3$**	**$AgNO_3$**
5mM to 20mM	24	96	12	12
5mM to 40mM	24	96	6	6
5mM to 80mM	6	24	6	6
10mM to 20mM	60	60	24	24
10mM to 30mM	12	6	6	6
10mM to 40mM	6	60	12	12
10mM to 80mM	12	24	6	6
10mM to 90mM	6	6	6	6

Table 4. **Organic linker 2,7-bis((4*H*-1,2,4-triazol-4-yl)methyl)phenanthrene used in conjunction with many group 11 metal salts. Results highlighted in red indicate conditions where crystals were grown and the numerical values indicated in this table are how many vials were set over the course of a year long period. Of the over 500 vials that were tested, there was no crystalline material that was synthesized on a large enough scale that could be used for SCXRD analysis.**

Concentrations of Ligand to Metal	$CuBr_2$	$CuCl_2$	$CuNO_3$	$AgNO_3$
5mM to 20mM	24	96	12	12
5mM to 40mM	24	96	6	6
5mM to 80mM	6	24	6	6
10mM to 20mM	60	60	24	24
10mM to 30mM	12	6	6	6
10mM to 40mM	6	60	12	12
10mM to 80mM	12	24	6	6
10mM to 90mM	6	6	6	6

purple all of which represented either the presence of an excess metal center, a reduced metal center, or a hypothesized desirable powder. In these many samples obtained, not one had given a large enough crystal sample for running on SCXRD. Small crystalline material was obtained, but with the material being either too short, too thin, or too brittle, no conclusive evidence could be obtained to date. Utilizing collaborative work with the Gianneschi group, it may be possible in the future to utilize the Rigaku Synergy-ED micro electron diffractor which could in theory visualize these extremely small crystals.[6,7]

Conclusions

The synthesis of MONTs can be broken into two equally as important segments, the first being an organic segment and the second being an inorganic segment. With these considerations in mind, attempting to synthesize MONTs with many different organic linkers and group 11 metal salts was necessary. In this chapter, initial attempts to synthesize a MONT with an expanded pore resulted in a "mixed bag" of results which ranged from conclusive to inconclusive. Using organic linker 4,4"-bis((4*H*-1,2,4-triazol-4-yl)methyl)-1,1':3',1"-terphenyl and $CuCl_2$ a MONT was synthesized with a resulting pore width of 17.5Å which can be considered one of the largest pored MONTs ever made when using the two-column pillared approach. Multiple routes for synthesis based on alternating concentrations are being currently reviewed for the future of expanded pore MONT development. Although all work indicated in this chapter did not lead to a full portfolio of expanded MONTs, it did lead to the discovery of a novel MONT, a preliminary MOF, and a plan for the analysis of much smaller crystals. With this provided information, the future of synthesizing two-column pillared MONTs with an expanded pore has been further paved and developed.

Experimental

Synthesis of Cu_2(4,4''-bis((4*H*-1,2,4-triazol-4-yl)methyl)-1,1':3',1''-terphenyl)Cl_2 (MONT): To a clean, dry, 20 mL vial 39.9 mg of 4,4''-bis((4*H*-1,2,4-triazol-4-yl)methyl)-1,1':3',1''-terphenyl was added to 10mL of dimethylformamide creating a stock solution with a 10 mM concentration. To a second clean, dry, 20 mL vial 138 mg of $CuCl_2$ was dissolved in 10 mL of water creating an 80 mM stock solution. From this point, multiple different reaction ratios were made based on doing a series of sample dilutions (***Table 1***). From the bulk phase solution of **1d**, simple dilutions were made to generate concentrations suitable for MONT reactions i.e. 0.25 mL of **1c** stock solution was diluted with 0.75 mL of DMF in order to form a 2.5 mM solution. Similarly, $CuCl_2$ concentrations suitable for MONT reactions were generated by simple dilutions, i.e. a 0.25 mL aliquot of stock $CuCl_2$ solution was diluted with 0.75 mL of water to form a 20 mM solution. Reaction conditions yielding the highest rate of success consisted of 10 mM solution of **1a** to 40 mM $CuCl_2$ solution with a volumetric ratio of 1:1 and a total volume of 2 mL. Reaction mixtures were sealed, mixed, and heated to 85 °C undisturbed for 2 weeks, after which the resulting crystal grown was bulky, large, and had a green hue. The crystals were isolated *via* filtration, washed with 5x2 mL of 40 °C hot acetone and then washed with 5x2 mL of 80 °C water. Multiple samples were collected of visually similar crystals to be used for various bulk phase PXRD and IR analysis. IR: 3394, 3112, 1980, 1663, 1540, 1514, 1444, 1395 ,1340 ,1255 ,1213, 1185, 1080, 1010, 854, 788, 754, 700, 662, 611, 588, 556 cm^{-1}.

Synthesis of Cu_2(bis(4-((4*H*-1,2,4-triazol-4-yl)methyl)phenyl)methane)Cl_2 (MOF): To a clean, dry, 20mL vial 33.4 mg of bis(4-((4*H*-1,2,4-triazol-4-yl)methyl)phenyl)methane was added to 10mL of dimethylformamide creating a stock solution with a 10mM concentration. To a second clean, dry, 20mL vial 105 mg of $CuCl_2$ is added to 20mL of water creating a stock

solution with an 30mM concentration. For the synthesis with the highest success, a 10mM to 90mM solution with a volumetric ratio of 1:3 was mixed and ran in triplicate multiple times. Heated to 85°C and set aside for 2 days, the resulting crystal grown was bulky, star shaped, and clear. Multiple samples were collected of visually similar crystals to be used for bulk phase PXRD and IR analysis. Similar conditions discussed in the synthesis of Cu_2(4,4"-bis((4*H*-1,2,4-triazol-4-yl)methyl)-1,1':3',1"-terphenyl)Cl_2 were also tested, however the resulting crystals were too small for analysis on SCXRD (***Table 2)***. IR: 3440, 3116, 2285, 2163, 1979, 1660, 1606, 1539, 1508, 1476, 1445, 1420, 1392, 1353, 1333, 1210, 1177, 1117, 1075, 1024, 993, 886, 865, 849, 744, 735, 700, 690, 645, 631, 573, 558 cm^{-1}.

References

1. Jia, J.-G. and Zheng, L.-M. “Metal-Organic Nanotubes: Designs, Structures and Functions” *Coordination Chemistry Reviews* 403, **2020**: 213083.

2. Otsubo, K.; Wakabayashi, Y.; Ohara, J.; Yamamoto, S.; Matsuzaki, H.; Okamoto, H.; Nitta, K.; Uruga, T.; Kitagawa, H. Bottom-up realization of a porous metal–organic nanotubular assembly. *Nature Materials* **2011**, *10*, 291–295.

3. Vailonis, K. M., Gnanasekaran, K., Powers, X. B., Gianneschi, N. C., and Jenkins, D. M. Elucidating the Growth of Metal–Organic Nanotubes Combining Isoreticular Synthesis with Liquid-Cell Transmission Electron Microscopy *Journal of the American Chemical Society* 141, no. 26 **2019**, 10177–10182.

4. Murdock, C. R.; Jenkins, D. M. Isostructural Synthesis of Porous Metal–Organic Nanotubes. Journal of the American Chemical Society **2014**, 136 (31), 10983–10988.

5. Szuromi, P. Glimpsing growing nanotubes. *Science* **2019**, *365* (6450), 246.

6. Gnanasekaran, K.; Vailonis, K. M.; Jenkins, D. M.; Gianneschi, N. C. *In Situ* Monitoring of the Seeding and Growth of Silver Metal–Organic Nanotubes by Liquid-Cell Transmission Electron Microscopy. *ACS Nano* **2020**, *14* (7), 8735–5743.

7. Nalaoh, P. and Jenkins, D. M. “Di-Triazole Boat Conformation Leads to Metal–Organic Nanotube While Chair Conformation Leads to Coordination Polymer” *CrystEngComm* 25, no. 35 (**2023**): 4929–4933.

8. Jin, J.-C.; Wang, Y.-Y.; Liu, P.; Liu, R.-T.; Ren, C.; Shi, Q.-Z. An Unusual Independent 1D Metal−Organic Nanotube with Mesohelical Structure and 1D → 2D Interdigitation. *Crystal Growth & Design* **2010**, *10* (5), 2029–2032.

CHAPTER 4

SYNTHESIS OF PYRAZOLES FOR EXPANSION OF ORGANIC LINKER LIBRARY FOR METAL-ORGANIC NANOTUBES

Abstract

MONTs have been synthesized under many different approaches with the most popular approaches being the two-column, three-column, or four-column pillar. As the routes for synthesis of this subgroup of MOF continues to develop, the expansion of organic linkers that can be used to synthesize MONTs also increases. The studies discussed in this chapter tend to lean heavily into the future direction of MONT synthesis. For the future, many novel organic linkers are proposed, of which many have yet to be synthesized. These linkers proposed are di-pyrazole based linkers which in theory should lead to stronger bonding between the nitrogen bound within the pyrazole and a metal center. Considering new chemical conditions where an overall (-2) charge is highlighted, the use of group 9, 10, or 11 metal salts could be used to synthesize a new series of MONTs which would in turn expand the current portfolio of MONTs.

Introduction

As a key component to any porous material synthesis, organic linkers are used to provide overall structure and function. Published in literature, many different organic linkers have been used for the synthesis of MONTs. Beginning with the Kitagawa group, organic segments ethylenediamine and 4,4'-bipyridine were coordinated to a platinum center which formed one of the first examples of a four-column pillared MONT. Years later, the Jenkins group utilized di-triazoles which were coordinated to a group 11 metal center which formed the first examples of isoreticular 2-column pillared MONT. In 2016, the Wu group utilized organic linker 1,1'-(5-methyl-1,3-phenylene)bis(1H-imidazole) and 5-bromonicotinate (Brna) which had coordinated to a nickel center and provided one of the first examples of a three-column pillared MONT. With a handful of different approaches to MONT synthesis a lingering question has yet to be answered; "Which organic linkers could alleviate the issues of each approach, and how

could the positives of each approach be strengthened?". In this chapter, many organic linkers utilizing di-pyrazoles are discussed due to their stronger nature of bonding and their ability to have a more diverse portfolio of metals to bind to. Shown in ***Figure 24***, a series of organic linkers utilizing di-pyrazoles are proposed in which organic linkers (**L7-14**) could be theorized to produce MONTs within the three, four, or even two-column pillared category.[1-8] This being said, interactions between one nitrogen within the pyrazole ring would provide a stronger bond between the organic linker to a metal center which in turn would strengthen the formed crystalline material. To draw connections between di-triazole organic linkers and di-pyrazole organic linkers, **L15-19** (***Figure 24)*** shows many linkers with a similar structure but with the addition of methyl groups which provide planar stability.[9-11] Much of the work done in this chapter is based upon the adaption of many organic reactions which were modified to different synthetic schemes. To expand further, results provided are in the infantile stage, where very few reactions were successful. It is important to note, however, that the results that had failed also provided some important insights for the future of using di-pyrazoles as an organic linker for MONT synthesis.

Results and Discussion

Traditionally MONTs have been synthesized utilizing organic linkers that follow various common organic workups, however, in the case of using di-pyrazoles as an organic linker, many modifications to these common organic workups are necessary in order to form the desired organic linker. Various issues, primarily solubility and structural stability have resulted in this organic linker having little to no progress in the last many years of research. Pioneered by both Dr. Long and coworkers and Dr. Day and coworkers **L7** and **L15** (shown in ***Figure 24)*** are two of the very few di-pyrazole organic linkers that have been synthesized at a large enough

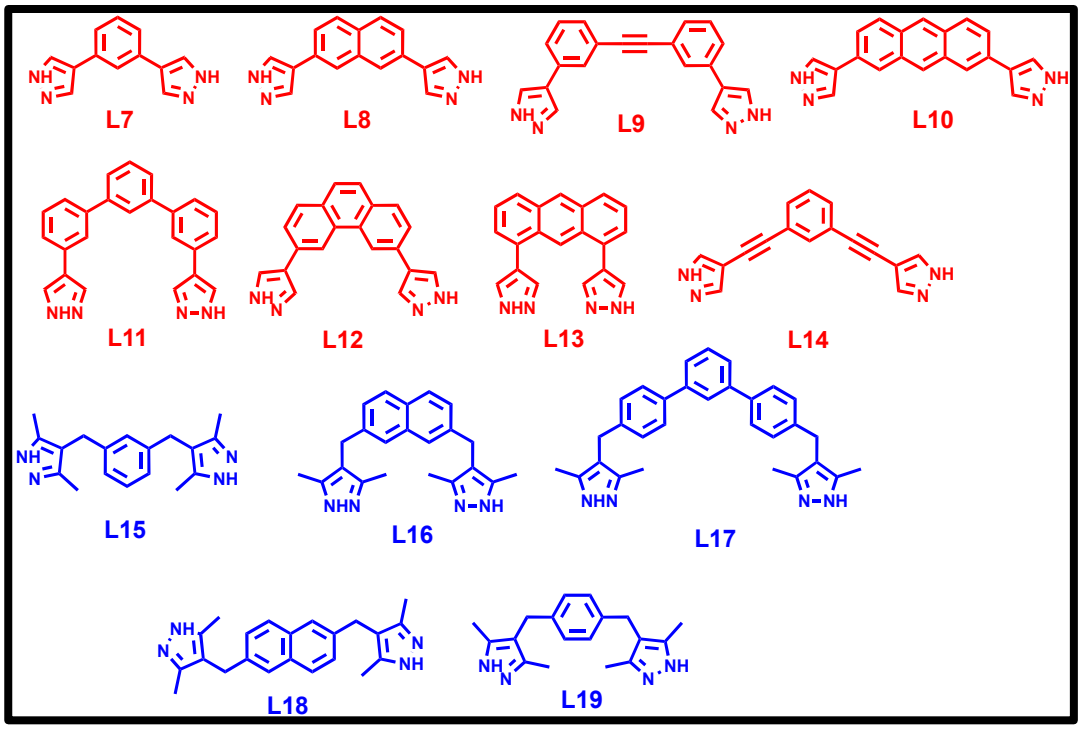

Figure 24. **A scheme of the proposed di-pyrazole ligands for MONT formation. L7-L10 will illustrate general pyrazole style MONT synthesis, L11-L14 will investigate pore size and geometric changes, and L15-L19 are most similar to Jenkins group style 1,2,4-ditriazole ligands for direct comparison.**

scale for analysis.[1-9] This chapter highlights the replicability of the work of these two pioneers while also diving into potential new ways for ligand design and future MONT synthesis. Shown in ***Figure 24***, 1,3-bis((3,5-dimethyl-1*H*-pyrazol-4-yl)methyl)benzene (**L15)** was utilized by Dr. Li and coworkers in 2019 which led to one of the first formed di-pyrazole MONTs. This crystal had a Cu_6(1,3-bis((3,5-dimethyl-1*H*-pyrazol-4-yl)methyl)benzene)$_3$ formula and was the pioneering result of one of the first three-column pillared MONTs where the ligand acted as both the main structural component and as the capping agent for closing the nanotube. It was this work that prompted the interest of other groups across the globe to investigate di-pyrazoles as an organic linker for MONT synthesis.[11] Prior to this, Dr. Long and coworkers in 2010 synthesized a di-pyrazole MOF utilizing organic linker 1,3-di(1*H*-pyrazol-4-yl)benzene (**L7)** and a Zn^{2+} metal center.[8] With published data suggesting the potential for di-pyrazoles as an organic linker for crystalline material synthesis, novel organic linkers were designed with the purpose of expanding the library of organic linkers which would, in theory, cause the size of the MONT portfolio as a whole to undergo a dramatic increase.

As an example, organic linker 1,3-bis((1*H*-pyrazol-4-yl)ethynyl)benzene (shown in ***Figure 25***) is used in conjunction with a M^{2+} metal center. This theoretically formed MONT could be predicted to follow a two-column pillared approach while also expanding the size of the developed MONTs pore when basing this solely on predicted bond angles. It is important to discern though that theory does not always follow experimental function. In order to tackle this hypothesis, a series of organic reactions were tested. Following the synthetic method of Dr. Long and coworkers, three separate attempts at the synthesis of 1,3-di(1*H*-pyrazol-4-yl)benzene as an organic linker were concluded.[8] Under nitrogen, phosphorous oxychloride was added to anhydrous dimethylformamide where this mixture was chilled in an ice bath to 0°C before a

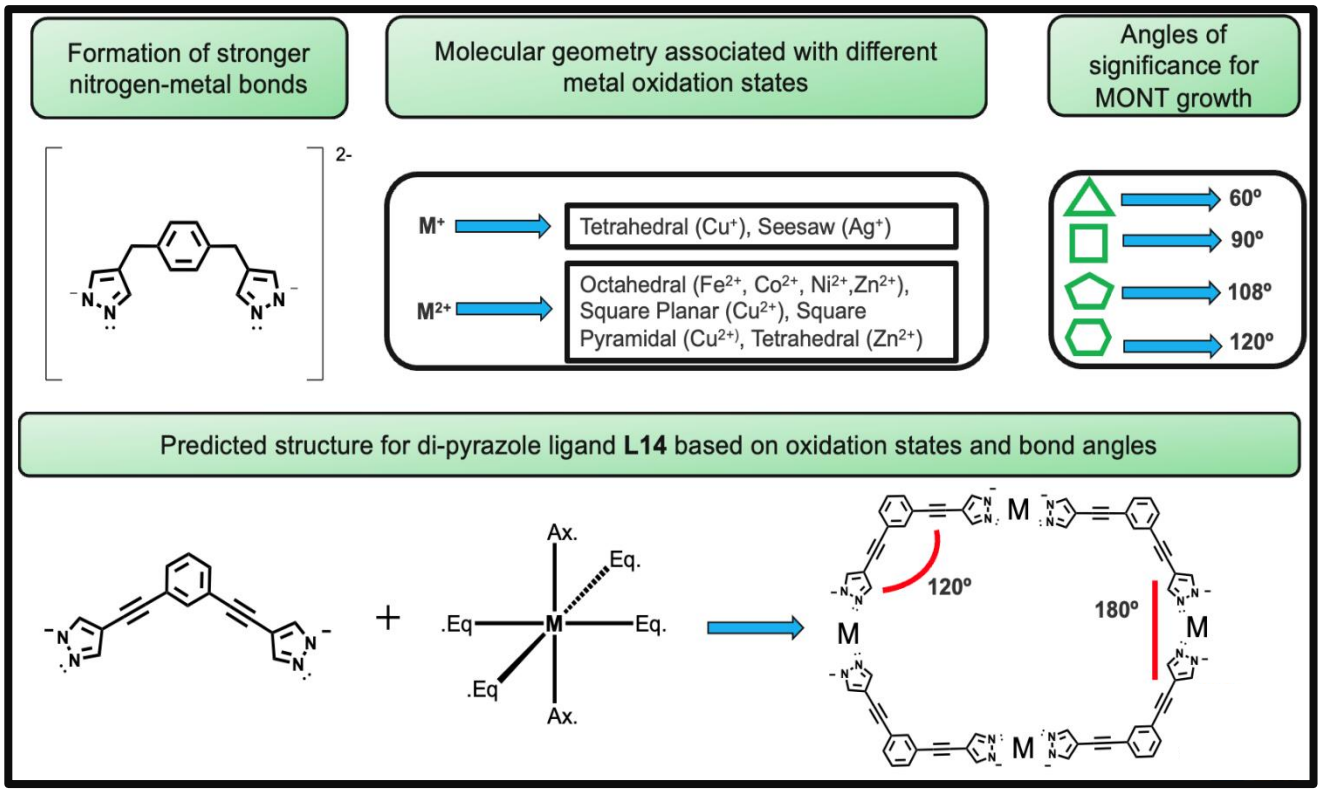

Figure 25. **Utilization of 1,3-bis((1*H*-pyrazol-4-yl)ethynyl)benzene with an M^{2+} octahedral metal center can be predicted to form a MONT structure with the supporting angles highlighted in red.**

solution of 1,3-phenylenedicarboxylic acid in dimethylformamide was added. This reaction mixture was heated to 70°C for 18 hours before continuation. While the solution was still hot, it was poured into a solution of ice water and sodium perchlorate resulting in an off white product.

This crude 1,3-benzenebis(2'-(1',3'-dimethylamino)-trimethinium diperchlorate was then rinsed with water, methanol, and diethyl ether resulting in a small amount of off white powder. During each rinse more and more crude was washed away resulting in ~5mg of crude product. This was not enough intermediate to continue the reaction, so this reaction was set twice more with similar outcomes resulting in ~10mg of product. With each reaction producing inconclusive results at a consistently abysmal yield, a different approach was taken which would utilize 1-trityl-1*H*-pyrazole as a protecting group, (similar to 3-(1H-1,2,4-triazol-1-yl)propanenitrile in the di-triazole systems). 1,4-bis(bromomethyl)benzene was stirred in a solution of DMSO, potassium tert-butoxide and 1-trityl-1*H*-pyrazole at 85°C for 16 hours. Utilizing different solvent systems ranging from 1:1, 1:4, and 1:20 hexanes/ethyl acetate for TLC, this reaction was monitored closely every 3 hours and spotted in comparison to the two starting materials. For the final spotting on TLC, no reaction was observed to have taken place, however, a bright, yellow crystalline byproduct was obtained. Similarly, under the same reactions conditions 1,3-bis(bromomethyl)benzene was used in order to see if a slight steric change would influence the reaction. Once again, as similar TLC results proved inconclusive this led to changing the temperature of the reaction to 60°C to see if this would influence the formation of the desired product. Unfortunately, upon completion of a 24 hour time frame, there was no reaction observed for either combination of organic linker with 1-trityl-1*H*-pyrazole.

Shown in ***Figure 26,*** there was one final reaction condition tested which led to interesting preliminary data. For the synthesis of 2,2'-(1,4-phenylenebis(methylene))dimalononitrile, *N*-

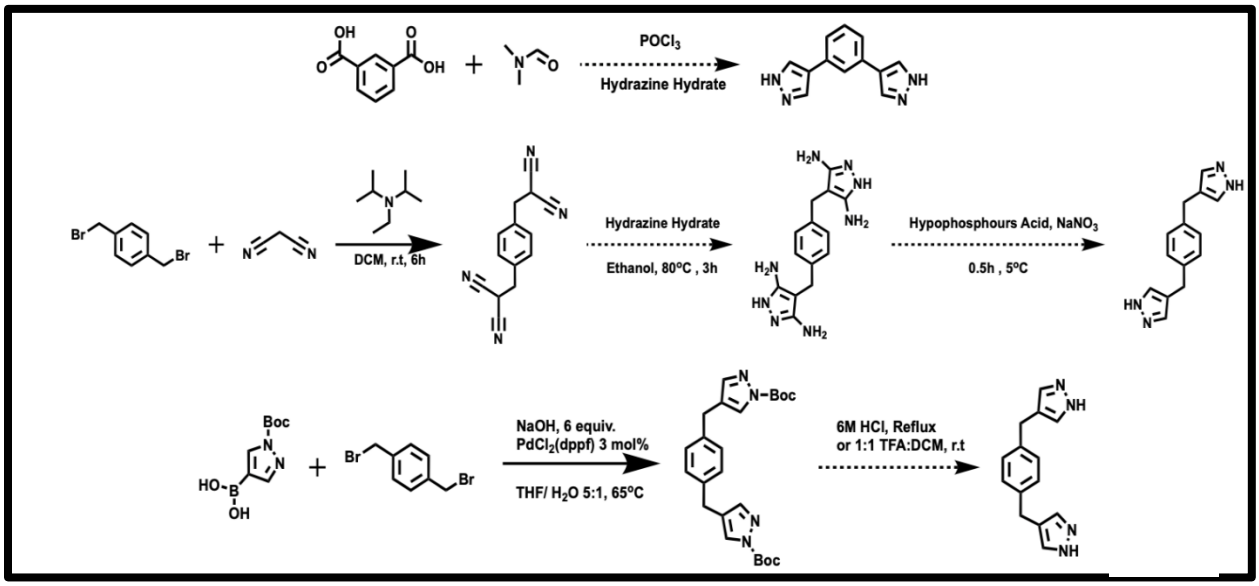

Figure 26. **Multiple reaction conditions were tested to determine the synthesis of di-pyrazole based organic linkers, but in each instance impurities, byproducts, or simply no reactions were observed.**

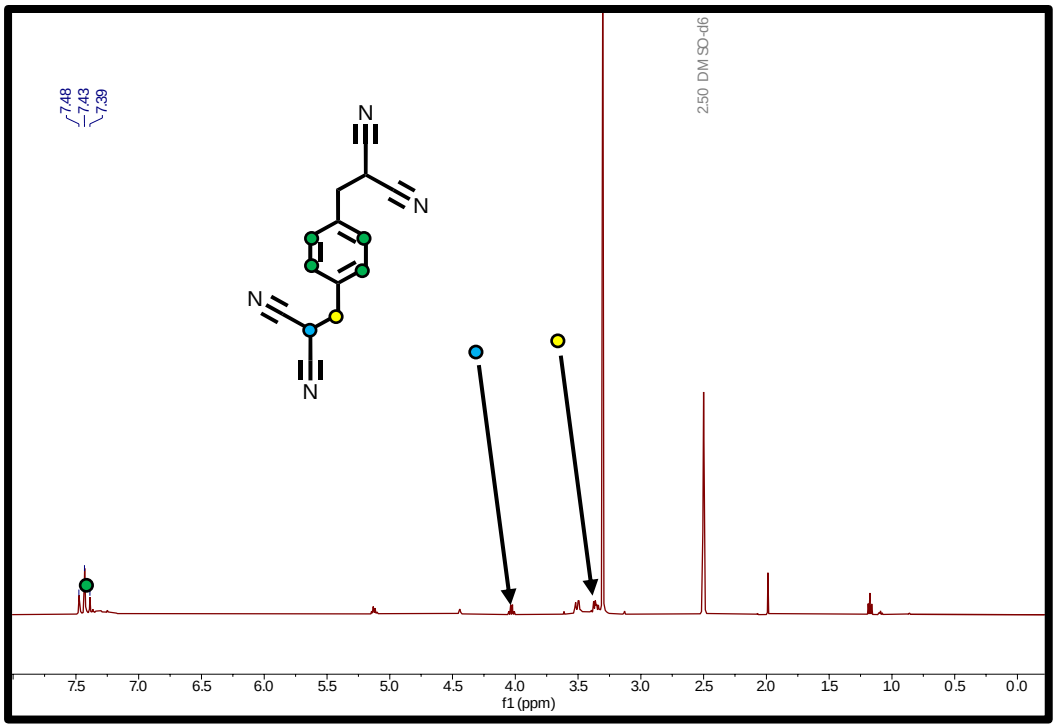

Figure 27. **^{1}H-NMR of crude 2,2'-(1,4-phenylenebis(methylene))dimalononitrile. Solvent and starting material residue to be purified via column, recrystallization, and drying.**

ethyl-*N*-isopropylpropan-2-amine and 1,4-bis(bromomethyl)benzene was added dropwise to a solution of malononitrile in dry dichloromethane at 0°C. This reaction mixture which was placed under nitrogen was allowed to reach room temperature before stirring for 6 hours. Quenching the solution using ice water, two separate phases were obtained. The organic layer was separated from aqueous, and ethyl acetate was added to the aqueous phase before separation. To this new organic ethyl acetate layer, brine was used to rinse before sodium sulfate was added to remove any present water. The final organic layer was decanted off, concentrated and purified via recrystallization using a combination of hexanes and ethyl acetate. Shown in ***Figure 27,*** a ^{1}H-NMR shows the desired final product of 2,2'-(1,4-phenylenebis(methylene))dimalononitrile, but further attempts at purification are required before continuation to future synthetic steps. A couple of other organic reactions were attempted for the synthesis of di-pyrazole organic linkers, but these are not listed as they either had no reaction, an unknown byproduct, or were synthesized at a scale too small to produce viable results.

Conclusions

MONTs can be synthesized utilizing a vast array of both ridgid and semi-ridgid organic linkers. Determining which organic linker to use in conjunction with a metal center is an important part of the development of these novel materials. As research progresses and the number of organic ligands that can be used for MONT synthesis grows, it in the future may be possible to use a more complex organic linker such as di-pyrazoles to alleviate restrictions of the three different approaches to MONT synthesis as discussed in this thesis. Within this chapter there were many complications which caused this project to be put on hold. The low reaction yields, low levels of purity, poor solubility and time constraints were all contributors to this project being moved to a future student. Di-pyrazoles are an interesting approach to alleviating

many restrictions of the various different pillared approaches. Whether that be for pore size or the use of different metal centers, the future of this project is currently undetermined, but with the complications discovered in this chapter it can be speculated that a future student will have this knowledge to refine this project further and grow it into something incredible.

Experimental

Synthesis of 1-trityl-1*H*-pyrazole: In a clean, dry, 500mL round bottom flask, 1H-pyrazole (6.00 g 88.13 mmol) were dissolved in 150 mL of dichloromethane and 12.5 mL triethylamine, then the flask was cooled to 0°C for 15 minutes, A solution of 27.02 g (96.94 mmol) trityl chloride in 100mL dichloromethane was then slowly added to the reaction mixture. This solution was stirred for 15 minutes at 0°C, warmed to room temperature, and stirred for 16 hours at room temperature. This solution was then washed with 50 mL of water, the organic layer was dried using magnesium sulfate, concentrated under vacuum, and product was purified via recrystallization in methanol. (25.42g, 84.0% yield) ^{1}H-NMR ($CDCl_3$, 499.74 MHz): σ 7.67 (s, 1H), 7.35 (m, J = 7.4 Hz , 10H), 7.16 (s, 6H), 6.25 (s, 1H). $^{13}C\{^{1}H\}$ NMR ($CDCl_3$, 125.67 MHz): σ 143.21, 139.54, 132.18, 130.02, 127.80, 127.54, 104.19, 78.38.

Synthesis of 2,2'-(1,4-phenylenebis(methylene))dimalononitrile: 780µL (4.50mmol) of *N*-ethyl-*N*-isopropylpropan-2-amine and 1.187g (4.50mmol) of 1,4-bis(bromomethyl)benzene was added dropwise under nitrogen to a solution of 300mg (4.50mmol) of malononitrile in dry dichloromethane at 0°C in a clean, dry 100 mL round bottom flask. The reaction mixture was warmed to room temperature and stirred for 6 hours. The reaction was quenched with 100 mL of ice water, yielding two phases. The mixture was taken up with 100 mL of ethyl acetate, separated, washed with 50 mL of brine, dried with sodium sulfate, and the product was purified via recrystallization from 100 mL of a 50/50 mixture of hexanes and ethyl acetate. (crude yield:

0.2363g, 25% yield)^{1}H-NMR (DMSO-d_6, 499.74 MHz): σ 7.43 (s, 4H), 4.10 (q, J = 3.9 Hz , 2H), 3.44 (d, J = 3.3 Hz , 4H). Other peaks present represent unreacted starting material and mono substituted product.

References

1. Shin, H. N. Novel Organic Electroluminescent Compounds and Organic Electroluminescent Device Using the Same (**2010**):

2. Shuyan, Y., Wang, Z., and Tong, J. Preparation of N-Containing Compound with Specific Response to Pressure Stimulation and Its Application in Photochemical Devices (**2021**):

3. Green, M. L. and Parkin, G. Application of the Covalent Bond Classification Method for the Teaching of Inorganic Chemistry *Journal of Chemical Education* 91, no. 6 (**2014**): 807–816.

4. Guédouar, H., Aloui, F., Beltifa, A., Ben Mansour, H., and Ben Hassine, B. Synthesis and Characterization of Phenanthrene Derivatives with Anticancer Property against Human Colon and Epithelial Cancer Cell Lines *Comptes Rendus Chimie* 20, no. 8 (**2017**): 841–849.

5. Liu, M., Li, S., Zhou, J., Zha, Z., Pan, J., Li, X., Zhang, J., Liu, Z., Li, Y., and Qiu, X. High-Yield Formation of Graphdiyne Macrocycles through on-Surface Assembling and Coupling Reaction *ACS Nano* 12, no. 12 (**2018**): 12612–12618.

6. Barton, D. H. R., Bévière, S. D., and Chavasiri, W. The Functionalization of Saturated Hydrocarbons. Part 25. Ionic Substitution Reactions in Goaggiv Chemistry: The Formation of Carbon-Halogen Bonds *Tetrahedron* 50, no. 1 (**1994**): 31–46.

7. Mio, M. J., Kopel, L. C., Braun, J. B., Gadzikwa, T. L., Hull, K. L., Brisbois, R. G., Markworth, C. J., and Grieco, P. A. One-Pot Synthesis of Symmetrical and Unsymmetrical Bisarylethynes by a Modification of the Sonogashira Coupling Reaction *Organic Letters* 4, no. 19 (**2002**): 3199–3202.

8. Choi, H. J., Dincă, M., Dailly, A., and Long, J. R. Hydrogen storage in Water-Stable Metal–Organic Frameworks Incorporating 1,3- and 1,4-Benzenedipyrazolate *Energy Environ. Sci.* 3, no. 1 (**2010**): 117–123.

9. Zhang, Q., Wang, B., Tan, J., Mu, G., Yi, W., Lv, X., Zhuang, S., Liu, W., and Wang, L. Optimized Electron-Transport Material Based on M-Terphenyl-Diphenylphosphine Oxide with the Harmonious Compatibility of High et and Electron Mobility for Highly Efficient Oleds *Journal of Materials Chemistry C* 5, no. 33 (**2017**): 8516–8526.

10. Chandrakumar, P. K., Dhiman, R., Woodward, C. E., Iranmanesh, H., Beves, J. E., and Day, A. I. Tiara[*n*]Uril: A Glycoluril-Based Macrocyclic Host with Cationic Walls *The Journal of Organic Chemistry* 84, no. 7 (**2019**): 3826–3831.

11. Zhan, S.-Z., Li, J.-H., Zhang, G.-H., Liu, X.-W., Li, M., Zheng, J., Ng, S. W., and Li, D. A Luminescent Edge-Interlocked Prismatic Heteroleptic Metallocage Assembled through a Ligand Replacement Reaction Chemical Communications 55, no. 80 (**2019**): 11992–11995.

CHAPTER 5

CONCLUSIONS

Thesis Summary

MONTs are a 1D porous material that are formed based on interactions between an organic linker, a metal center, and an anionic capping agent. The development of this subcategory of MOF can be accredited back to the early 2000s where many principal investigators created this novel class of material. MONTs as a whole have been developing at a rapid rate when compared to previous years, and with the collaborations of scientists worldwide, the future of this material has seemingly endless possibilities.

During my tenure at the University of Tennessee-Knoxville, creating a MONT with a pore larger than those formed during the time of my predecessors was a primary goal. Utilizing organic linkers 4,4"-bis((4*H*-1,2,4-triazol-4-yl)methyl)-1,1':3',1"-terphenyl and bis(4-((4*H*-1,2,4-triazol-4-yl)methyl)phenyl)methane in conjunction with the group 11 metal salt $CuCl_2$, both conclusive and preliminary data was acquired using analytical methods of SCXRD, PXRD, TGA, and Gas adsorption. The findings included within this thesis had successfully proven that when expanding the size of an organic di-triazole linker, it was possible to see an increase upwards of 50% in the overall width of the developed MONT. As a secondary minor goal, the organic linker library for MONT synthesis was targeted for expansion. With results discussed in Chapter 4, although there were many reactions that resulting in the realm of the unknown, the outcomes of said experimentation have provided to being a useful foundation for the potential continuation of using di-pyrazoles as an organic linker for the synthesis of MONTs.

As MONTs with various different functions and forms continue to be developed, the use of both ridgid and semi-ridged organic linkers becomes more attractive. The development of organic linkers that can from bonds with multiple different metal groups on the periodic table can

aid in the alleviation of certain synthetic restrictions and the continued growth for this class of material.

VITA

Patrick Flavin Luciani was born on May 5, 2000 in Fort Myers, Florida to Patricia and John Luciani. He was raised in Pace, Florida where he graduated from Pace High School in 2018, then received a scholarship to attend the University of West Florida where he studied biochemistry. During his time at West Florida, he was a member of the Honors College, was involved with many student organizations, participated in four research groups, and went to a conference at the National Sea-Phages symposium in Tampa, Florida. He completed his bachelor's degree of biochemistry in 2022 and two weeks later moved to Knoxville, Tennessee to start his graduate degree early at the University of Tennessee-Knoxville. Patrick began to work under the tutelage of Dr. David Jenkins early on in his first fall semester of graduate school where he primarily focused on the synthesis of metal organic nanotubes and expanded organic linkers.